environmental microbiology

Environmental Microbiology (2020) **00**(00), 00–00 doi:10.1111/1462-2920.14903

Environmental conditions steer phenotypic switching in acute hepatopancreatic necrosis disease-causing *Vibrio parahaemolyticus*, affecting PirA^{VP}/PirB^{VP} toxins production

Vikash Kumar,[1,2*] **Suvra Roy**,[1,2] **Kartik Baruah**,[1,3] **Delphi Van Haver**,[4,5,6] **Francis Impens**[4,5,6] **and Peter Bossier**[1]

[1]*Laboratory of Aquaculture & Artemia Reference Center, Faculty of Bioscience Engineering, Department of Animal Sciences and Aquatic Ecology, Ghent University, 9000, Ghent, Belgium.*

[2]*ICAR – Central Inland Fisheries Research Institute (CIFRI), Barrackpore, 700120, India.*

[3]*Department of Animal Nutrition and Management, Faculty of Veterinary Medicine and Animal Sciences, Swedish University of Agricultural Sciences, Uppsala, 75007, Sweden.*

[4]*VIB-UGent Center for Medical Biotechnology, B-9000, Ghent, Belgium.*

[5]*Department of Biomolecular Medicine, Ghent University, B-9000, Ghent, Belgium.*

[6]*VIB Proteomics Core, B-9000, Ghent, Belgium.*

Summary

Bacteria in nature are widely exposed to differential fluid shears which are often a trigger for phenotypic switches. The latter mediates transcriptional and translation remodelling of cellular metabolism impacting among others virulence, antimicrobial resistance and stress resistance. In this study, we evaluated the role of fluid shear on phenotypic switch in an acute hepatopancreatic necrosis disease (AHPND)-causing *Vibrio parahaemolyticus* M0904 strain under both *in vitro* and *in vivo* conditions. The results showed that *V. parahaemolyticus* M0904 grown at lower shaking speed (110 rpm constant agitation, M0904/110), causing low fluid shear, develop cellular aggregates or floccules. These cells increased levan production (as verified by concanavalin binding) and developed differentially stained colonies on Congo red agar plates and resistance to antibiotics. In addition, the phenotypic switch causes a major shift in the protein secretome. At 120 rpm (M0904/120), PirA^{VP}/PirB^{VP} toxins are mainly produced, while at 110 rpm PirA^{VP}/PirB^{VP} toxins production is stopped and an alkaline phosphatase (ALP) PhoX becomes the dominant protein in the protein secretome. These observations are matched with a very strong reduction in virulence of M0904/110 towards two crustacean larvae, namely, *Artemia* and *Macrobrachium*. Taken together, our study provides substantial evidence for the existence of two phenotypic forms in AHPND *V. parahaemolyticus* strain displaying differential phenotypes. Moreover, as aerators and pumping devices are frequently used in shrimp aquaculture facilities, they can inflict fluid shear to the standing microbial agents. Hence, our study could provide a basis to understand the behaviour of AHPND-causing *V. parahaemolyticus* in aquaculture settings and open the possibility to monitor and control AHPND by steering phenotypes.

Introduction

Microorganisms have evolved to survive in variable and at times extreme conditions and by changing their phenotype they mount an effective response to environmental heterogeneity (Fonseca and Sousa, 2007; Guo and Gross, 2014; Kent *et al*., 2018). Aquatic bacteria are often subjected to fluid shear and hydrodynamic forces, created by either natural factors or anthropogenic activities like use of aerators or blowers to enhance shrimp productivity (Sultana *et al*., 2017; Welker *et al*., 2019). Yet any change in fluid shear or shaking growth condition might trigger phenotype switching and induce remodelling of transcription and translational networks which can determine virulence, antimicrobial resistance and persistence of a bacteria in hostile environment based on the creation of several variants equipped to adapt and maintain cellular status (Scott *et al*., 2010; Park *et al*., 2011; Sousa *et al*., 2011; Thomen *et al*., 2017).

Received 21 October, 2019; revised 12 December, 2019; accepted 18 December, 2019. *For correspondence. E-mail vikash.kumar@ugent.be

The Gram-negative marine bacterium, *Vibrio parahaemolyticus* M0904 strain is an important aquatic pathogen and capable of causing acute hepatopancreatic necrosis disease (AHPND) and several other important diseases in shrimp aquaculture (Li *et al*., 2017). The shrimp production in AHPND-affected regions has at times dropped considerably (to ~60%), and disease has caused a global loss of $1 billion per year to the shrimp farming industry (Nunan *et al*., 2014; Lee *et al*., 2015). The *V. parahaemolyticus* M0904 strain contains a pVA1 plasmid (63–70 kb) encoding the binary toxins named $PirA^{VP}$ and $PirB^{VP}$ homologous to the *Photorhabdus luminescens* insect-related (Pir) toxins PirA/B (Han *et al*., 2015; Campa-Córdova *et al*., 2017). The $PirA^{VP}$ and $PirB^{VP}$ toxins are the primary virulence factor of AHPND-causing bacteria involved in AHPND pathogenesis and mortality in shrimps (Han *et al*., 2015; Campa-Córdova *et al*., 2017; Dong *et al*., 2017).

In our previous studies, the *V. parahaemolyticus* M0904 AHPND strain and $PirA^{VP}$ and $PirB^{VP}$ secreted toxins have been reported to cause mortality in shrimp (Kumar *et al*., 2018; 2019b; Roy *et al*., 2019). However, in subsequent preliminary studies, results showed that *V. parahaemolyticus* cells grown at lower shaking speed (110 rpm) produced floccules which apparently displayed reduced virulence towards shrimp species. These preliminary results suggested that *V. parahaemolyticus* might display distinct phenotypes depending on fluid shear or shaking growth conditions. Here, for the first time, it is demonstrated that low fluid shear growth conditions can trigger phenotype switching in *V. parahaemolyticus*, mediating, among others, changes such as biofilm formation and antibiotic resistance. Furthermore, it was also noted that *V. parahaemolyticus* at lower shaking speed downregulates $PirA^{VP}$/$PirB^{VP}$ toxins expression while producing and secreting an alkaline phosphatase (ALP) PhoX.

Results

V. parahaemolyticus *(strain M0904) grown at low shaking speed conditions flocculates and makes biofilm*

At first, the effect of shaking speed on *V. parahaemolyticus* M0904 strain was examined considering that altered environmental conditions might modulate the bacterium and trigger a set of adaptive regulatory mechanisms (Balaban *et al*., 2004; Van Der Woude, 2006; Rossignol *et al*., 2009). The results showed that *V. parahaemolyticus* cells incubated at constant agitation of 110 rpm (later on called M0904/110) flocculated, whereas cells grown at 120 rpm (later on called M0904/120) did not produce floccules (Fig. 1A). This indicated that low shaking speed induces flocculation in *V. parahaemolyticus* culture.

Next, the significance of shaking speed and floccules production on biofilm formation was determined, because microorganisms in altered environmental conditions are often able to switch phenotype and form biofilm (Dewanti and Wong, 1995; Leid *et al*., 2002; Fonseca and Sousa, 2007; Zhou *et al*., 2014). To this end, the biofilm formation of M0904/110 and M0904/120 were compared in Erlenmeyer flasks using the tube method. M0904/110 showed significantly higher biofilm formation (approximately fourfolds) as compared with M0904/120 (Fig. 1B).

Detection of V. parahaemolyticus *M0904 strain cellular structures and changes associated with shaking speed*

To further dissect the effect of shaking conditions, the *V. parahaemolyticus* M0904 cells (either M0904/110 or M0904/120) were analysed by microscopy. Under light microscopy analysis, the results showed that M0904/110 cells indeed form cellular aggregates (Fig. 2i – A and B). Moreover, M0904/120 cells displayed mostly singular cells (Fig. 2i – E and F). As extracellular polymeric substances (EPSs), composed of various sugar polymers, play a significant role in the formation of cellular aggregates or floccules (Vuong *et al*., 2004), EPS production in M0904/110 cellular aggregates was examined. M0904/110 cells, stained with calcofluor, displayed more prominent exopolysaccharide production as compared with M0904/120 cells (Fig. 2i – C and D). The study therefore indicates that *V. parahaemolyticus* cultured in lower shaking condition produces EPS, a key component of cellular aggregates or floccules (Watnick, 2000; Hawkins and Geddes, 2017).

Seven different types of fluorescent-labelled lectins (with non-covalent specific binding to carbohydrates) were used to characterize the EPS produced (Leriche *et al*., 2000; Mlouka *et al*., 2016). Flow-cytometry analysis showed that concanavalin A (ConA) gave the highest fluorophore count in M0904/110 (Fig. 2ii – A and C). Moreover, there was no difference in the size of bacterial cells in either M0904/110 or M0904/120 (Fig. 2ii – B and D). Because ConA is known to bind with levan, a major exopolysaccharide produced by Gram-negative bacteria, these results suggest that *V. parahaemolyticus* strain grown at lower shaking speed produce levan in the cellular aggregates or floccules (Laue *et al*., 2006).

The evaluation of Congo red agar-based phenotype characteristics is a standard method developed to assess the *in vitro* slime production ability of bacteria. The development of purple-black colonies interpreted as positive biofilm-producing phenotype, while red colonies demonstrated as negative biofilm-producing phenotype (Freeman *et al*., 1989; Mariana *et al*., 2009; Phuoc *et al*., 2009). Hence, to further study the phenotype switch occurring in *V. parahaemolyticus* M0904 when grown at

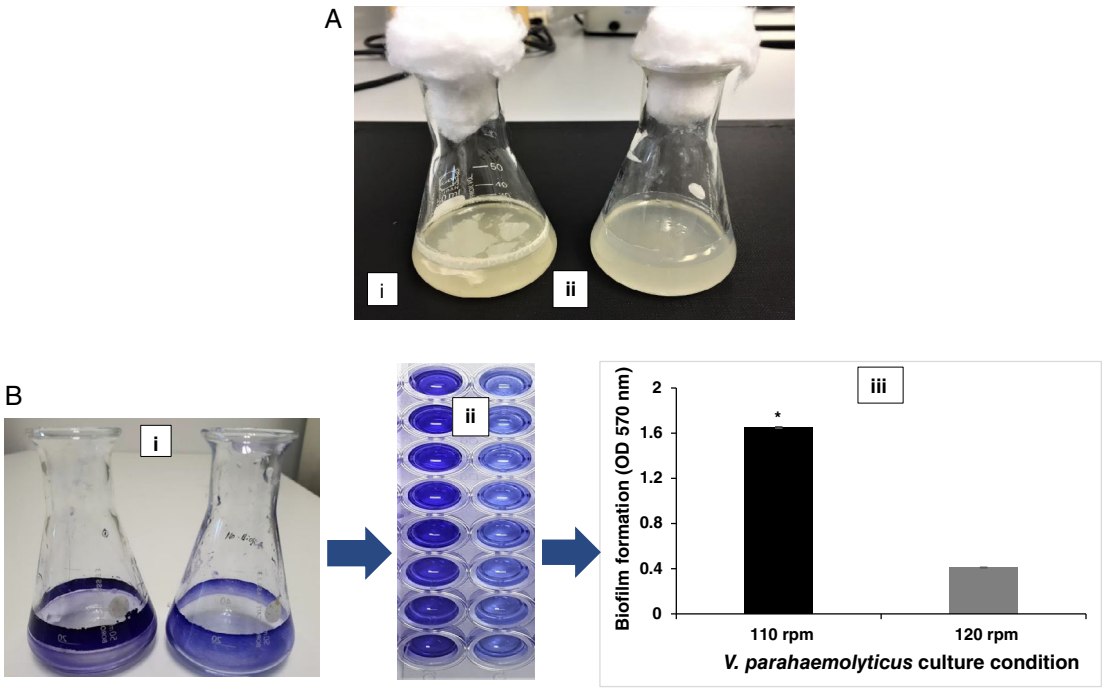

Fig. 1. The *Vibrio parahaemolyticus* M0904 strain grown in lower shaking speed condition induce flocculation and biofilm formation.
A. The *V. parahaemolyticus* M0904 culture incubated overnight in 20 ml MB, (i) constant agitation at 110 rpm displays high flocculation (M0904/110); (ii) constant agitation at 120 rpm exhibits no floccule formation (M0904/120).
B. Detection and quantification of biofilm formation from *V. parahaemolyticus* M0904 strain under different culture conditions. (i, ii) The M0904/110 has higher biofilm formation on the walls and bottom of culture tubes as compared with M0904/120. (iii) Absorbance at 570 nm from M0904 strain M0904/110 or M0904/120 to quantify the biofilm formation.
Error bars represents standard error of three replicates. Asterisks represent significant a difference between the M0904/110 or M0904/120 * ($P < 0.001$).

lower shaking condition, M0904/110 and M0904/120 cells were grown on marine agar with Congo red (MACR) plates, and colonies were compared for differential staining. Interestingly, M0904/110 culture that produces floccules developed purple colonies on MACR plates, while the M0904/120 culture resulted in orange-red colonies (Fig. 2iii, A and B). This colour change, together with higher exopolysaccharide and ConA production, confirms that the EPS production is modified under low shaking conditions.

Floccule formation increases the resistance of AHPND V. parahaemolyticus *M0904 strain to antibiotics*

There is some evidence suggesting that phenotypic switching may be involved in microbes in developing resistance to chemotherapy (NCCLS, 2002; Kemper *et al*., 2014; CLSI, 2015). To test this hypothesis, the antibiotic susceptibility of M0904/110 or M0904/120 was examined against five different antibiotics, that is, kanamycin, ampicillin, rifampicin, tetracycline and chloramphenicol. The results showed that M0904/110 cells displayed resistance to kanamycin, ampicillin and rifampicin, while M0904/120 cells did not (Fig. S1). Although both cell types (M0904/110 or M0904/120) were sensitive to chloramphenicol, the clearing halos surrounding the antibiotic discs were significantly reduced in M0904/110 culture (Table 1). M0904/110 cells are hence displaying multiple antibiotic resistance under the described experimental conditions.

Flocculating cells no longer produce PirA^{VP} and PirB^{VP} toxins, but rather produce and secrete an ALP PhoX

As M0904/110 and M0904/120 cells display distinct phenotypic features at the level of EPS production, it was verified if secretion of proteins would be affected as well (Jayaraman, 2011; Sousa *et al*., 2011; Thomen *et al*., 2017). To investigate potential changes in the secretome, the proteins present in the ultrafiltrated culture supernatant from M0904/110 and M0904/120 cells [VP_{AHPND} extracellular protein (ECP)] were separated by SDS-PAGE and stained by Coomassie. This analysis showed that M0904/120 cells secrete two main proteins of 13 and 50 kDa, while M0904/110 cells secrete one prominent protein of 73 kDa, along with some other proteins that are differentially secreted by both cell types (Fig. 3A). Thus *V. parahaemolyticus* strain M0904 indeed changes

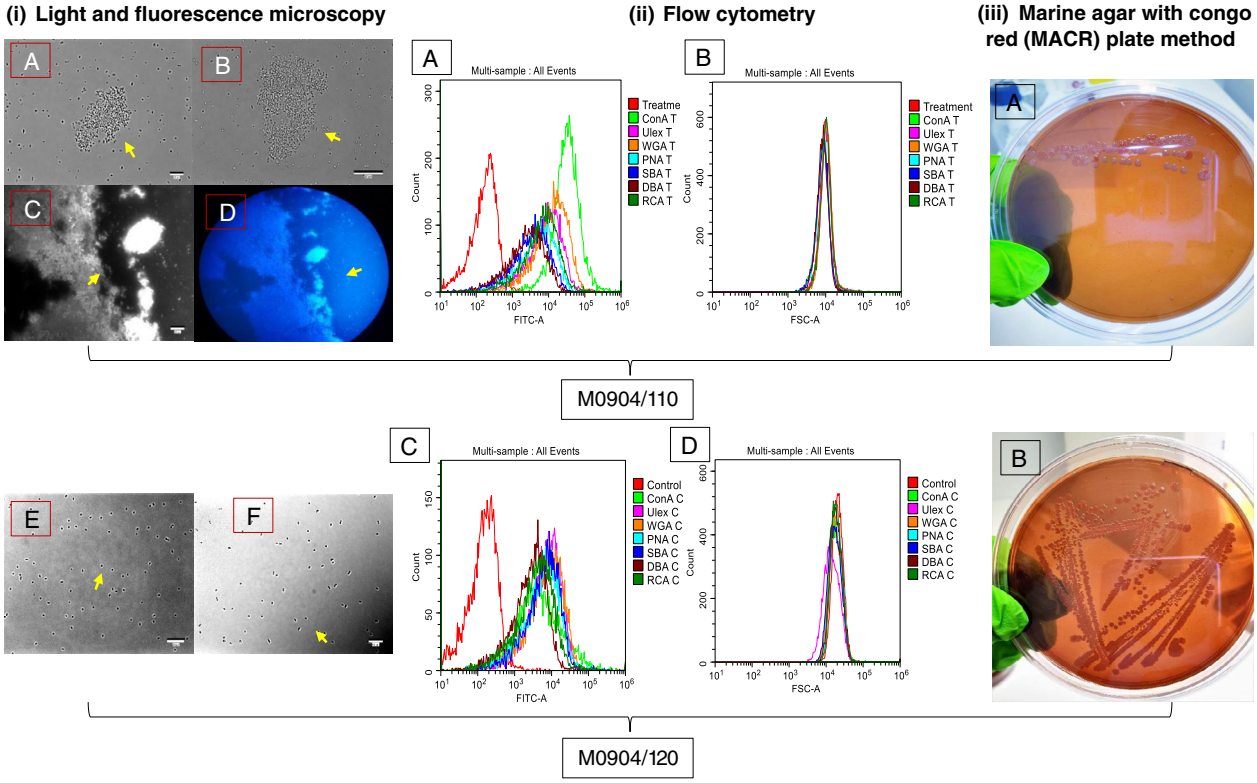

Fig. 2. Detection of *Vibrio parahaemolyticus* M0904 strain cellular structure and changes associated with shaking speed.
(i) Light and fluorescence microscopy: A, B, light microscopy images of *V. parahaemolyticus* cells incubated under constant agitation at 110 rpm (M0904/110); C, D, fluorescence microscopy images of floccules produced by M0904/110; E, F, light microscopy images of *V. parahaemolyticus* cells incubated overnight under constant agitation with 120 rpm (M0904/120).
(ii) Assessment of *V. parahaemolyticus* M0904 strain cellular structure and changes associated with shaking speed by flow cytometry. Based on glycan specificity, seven different types of lectins were used (ConA, Ulex, WGA, PNA, SBA, DBA, RCA) and labelled with *V. parahaemolyticus* cells: A, FITC-A/count histogram plot; B, FSC-A/count histogram plot from M0904/110; C, FITC-A/count histogram plot; D, FSC-A/count histogram plot from M0904/120. FITC-A/count-demonstrate the EPSs production in bacterial culture, FSC-A/count- shows the size of bacterial cells.
(iii) Congo red agar-based phenotypic characterization of *V. parahaemolyticus* M0904 strain: A, colonies of *V. parahaemolyticus* M0904 strain (M0904/110), exhibit purple colonies in Congo red agar plates; B, colonies of *V. parahaemolyticus* M0904 (M0904/120), display orange-red colonies in Congo red agar plates. The development of purple colony interpreted as positive biofilm producing phenotype, while red colonies demonstrated as negative biofilm producing.

the production of secreted proteins upon slight variation of shaking speed conditions.

Next, to identify the main secreted proteins, corresponding protein bands at 13, 50 and 73 kDa were excised from the gel and subjected to mass spectrometry analysis. (The mass spectrometry proteomics data have been deposited to the ProteomeXchange Consortium via the PRIDE partner repository with the data set identifier PXD015617.) This analysis identified the two main proteins produced by M0904/120 cells as PirA^{VP} (13 kDa) and PirB^{VP} (50 kDa),

Table 1. Mean values of antibiotic susceptibility of *Vibrio parahaemolyticus* culture with different shaking speed (mean ± standard error)

Antibiotic discs	Diameters of inhibition halos surrounding the discs (mm)		Zone diameter interpretive criteria (NCCLS, 2002; CLSI, 2015)	
	V. parahaemolyticus M0904/120	*V. parahaemolyticus* M0904/110	*V. parahaemolyticus* M0904/120	*V. parahaemolyticus* M0904/110
Kanamycin	15.40 ± 0.40^{b}	9.80 ± 0.66^{a}	Intermediate	Resistance
Ampicillin	18.20 ± 0.66^{b}	0^{a}	Sensitive	Resistance
Rifampicin	28.8 ± 0.48^{b}	14.4 ± 0.50^{a}	Sensitive	Resistance
Tetracycline	0	0	Resistance	Resistance
Chloramphenicol	34.60 ± 0.97^{b}	21 ± 0.70^{a}	Sensitive	Sensitive

Significant differences between 120 and 110 rpm constant agitation culture groups are indicated with different alphabets in superscript. Susceptibility of the AHPND *V. parahaemolyticus* strain to different antibiotics is expressed as sensitive (S), intermediate (I) and resistant (R) following the guidelines of the Clinical and Laboratory Standards Institute (NCCLS, 2002; CLSI, 2015).

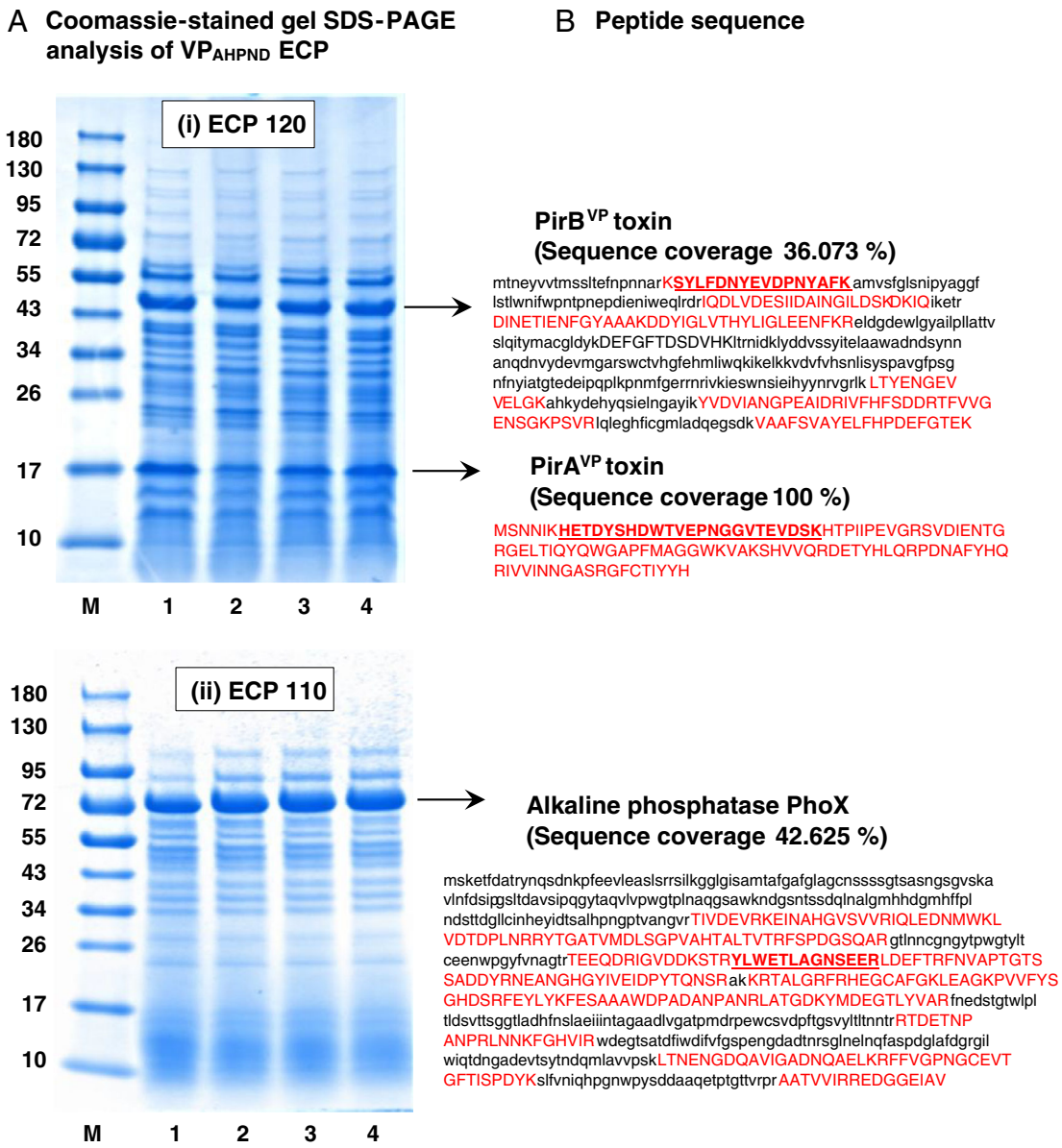

Fig. 3. Floccules formation associated with lower shaking speed attenuates PirA^{VP} and PirB^{VP} toxins production and enhances production of ALP PhoX in *Vibrio parahaemolyticus* M0904 culture.
A. Coomassie-stained SDS-PAGE gel of *V. parahaemolyticus* ECPs (VP$_{AHPND}$ ECPs). (i) ECP 120 shows two prominent bands at 13 and 50 kDa (lanes 1–4, showing the results of four replicate cultures). (ii) ECP 110 exhibits a single prominent band at 73 kDa (lanes 1–4, showing the results of four replicate cultures).
B. Two main proteins produced by ECP 120 (M0904/120) were identified as PirA^{VP} (13 kDa) and PirB^{VP} (50 kDa). The main protein secreted by ECP 110 (M0904/110) was identified as ALP PhoX with a molecular weight of 73 kDa.

the bacterial toxins encoded by a pVPA1 plasmid of AHPND *V. parahaemolyticus* strain (Han *et al*., 2015) (Fig. 3B). The main protein secreted by M0904/110 cells was identified as PhoX, an ALP with a molecular weight of 73 kDa (Figs 3B and S2, Table S1). These results suggest that M0904/110 cells stop producing PirA^{VP}/PirB^{VP} toxins and produce another secreted protein with tentative ALP activity, which might be playing important role in maintaining sufficiently high inorganic phosphorus level in the extracellular microenvironment to promote biofilm formation (Danikowski and Cheng, 2018).

ALP PhoX associated with floccules formation exhibits phosphate-solubilizing activity

It was verified whether the PhoX protein has phosphate-solubilizing activity. Hence, the bacterial suspensions of

V. parahaemolyticus (M0904/110 and M0904/120) were examined for phosphate-solubilizing activity in a Pikovskayas agar plate assay. As expected, the wells filled with M0904/110 cells produced a prominent phosphate-solubilizing zone as compared with wells incubated with M0904/120 cells (Fig. 4A). However, it may be noted that apart from PhoX, *V. parahaemolyticus* may produce other ALPs or phosphatase enzymes which could contribute to the phosphate-solubilizing activity (e.g. cell-bound phosphatase). Therefore, the phosphate-solubilizing activity of ECP was examined by two alternative approaches. At first phosphate-solubilizing activity was examined in wells filled with VP_{AHPND} ECP containing either ALP PhoX or $PirA^{VP}$ and $PirB^{VP}$ toxins. The results showed that ECPs secreted by M0904/110 display a phosphate-solubilizing zone as compared with secreted ECPs from M0904/120 (Fig. 4B). Later, the results were further verified to confirm the phosphate-solubilizing activity of purified PhoX and $PirA^{VP}$ and $PirB^{VP}$ proteins mixture using Pikovskayas agar plate assay. Again, wells filled with purified PhoX exhibited clear phosphate-solubilizing zone around the well. However, no activity was observed in the wells filled with purified $PirA^{VP}$ and $PirB^{VP}$ toxins (Fig. 4C). Together, these results show that M0904/110 cells secrete an ALP PhoX with demonstrable phosphate-solubilizing activity.

Floccules formation attenuates the expression of flagella-related motility genes and toxin genes in V. parahaemolyticus *M0904 strain*

Because there exists a correlation between flagellar motility and virulence of bacterial pathogens (Watnick, 2000; Hawkins and Geddes, 2017), the temporal difference in the expression of flagellar motility genes in *V. parahaemolyticus* (M0904/110 or M0904/120) was investigated at the transcriptional level. The selection of genes was based on the knowledge on flagellar motility in *V. parahaemolyticus*, the paradigm of flagellar motility in vibrios (Mccarter, 2004; Yang and Defoirdt, 2015). The results showed that expression of polar flagellin (*flaA*), chemotaxis protein (*CheR*) and polar flagellin-specific chaperone (*fliS*) gene were significantly decreased in M0904/110 as compared with the M0904/120 at the tested time points, namely, 12 and 24 h (Fig. 5A–C). The results suggest that *V. parahaemolyticus* at lower shaking speed modulate its behavior, reducing the transcription of flagellar motility genes.

To provide further evidence that M0904/110 decreased expression of virulence gene (as shown above), the transcription of pVA1 plasmid-bound genes, that is, $PirB^{VP}$ (responsible for $PirB^{VP}$ toxin)

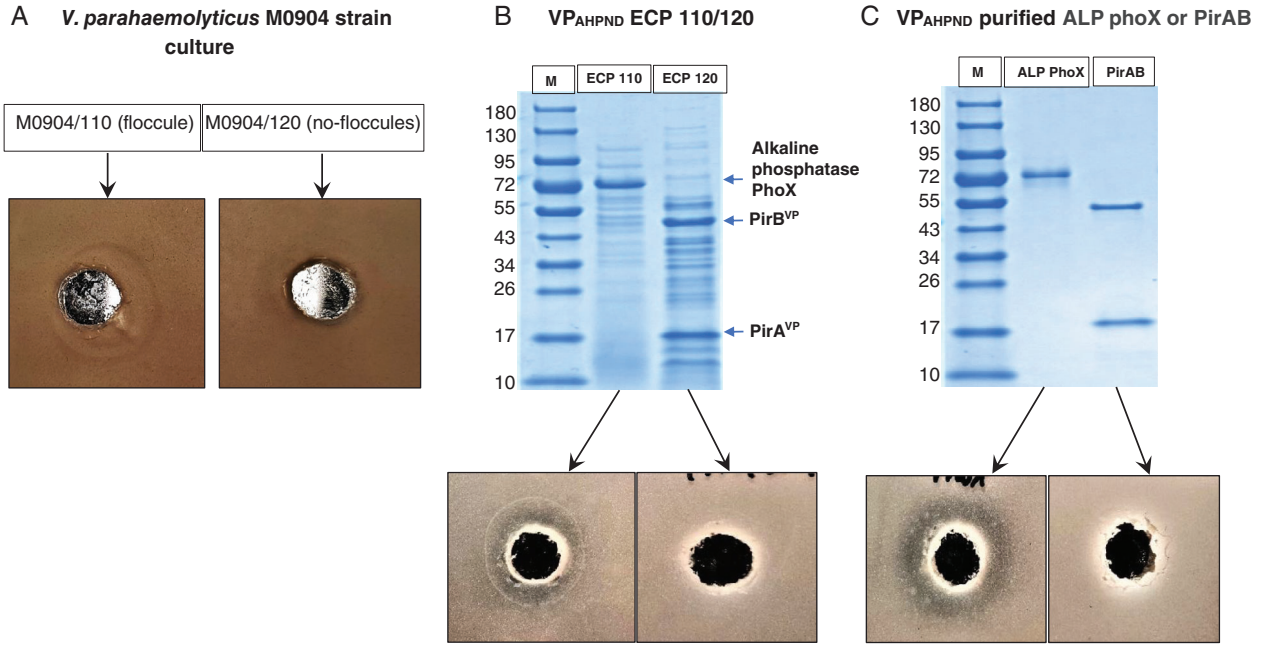

Fig. 4. ALP PhoX associated with floccules formation exhibits phosphate-solubilizing activity. *Vibrio parahaemolyticus* M0904 culture phosphate-solubilizing activity in Pikovskayas agar under different culture conditions.
A. The M0904/110 exhibits high phosphate-solubilizing activity in Pikovskayas agar plate assay, while M0904/120 display low phosphate-solubilizing activity.
B. VP_{AHPND} ECP 110 exhibits phosphate-solubilizing activity in Pikovskayas agar and VP_{AHPND} ECP 120 shows low phosphate-solubilizing activity.
C. VP_{AHPND} purified ALP phoX (ALP PhoX) display phosphate-solubilizing activity in Pikovskayas agar, while VP_{AHPND} $PirA^{VP}$/$PirB^{VP}$ exhibit no phosphate-solubilizing activity.

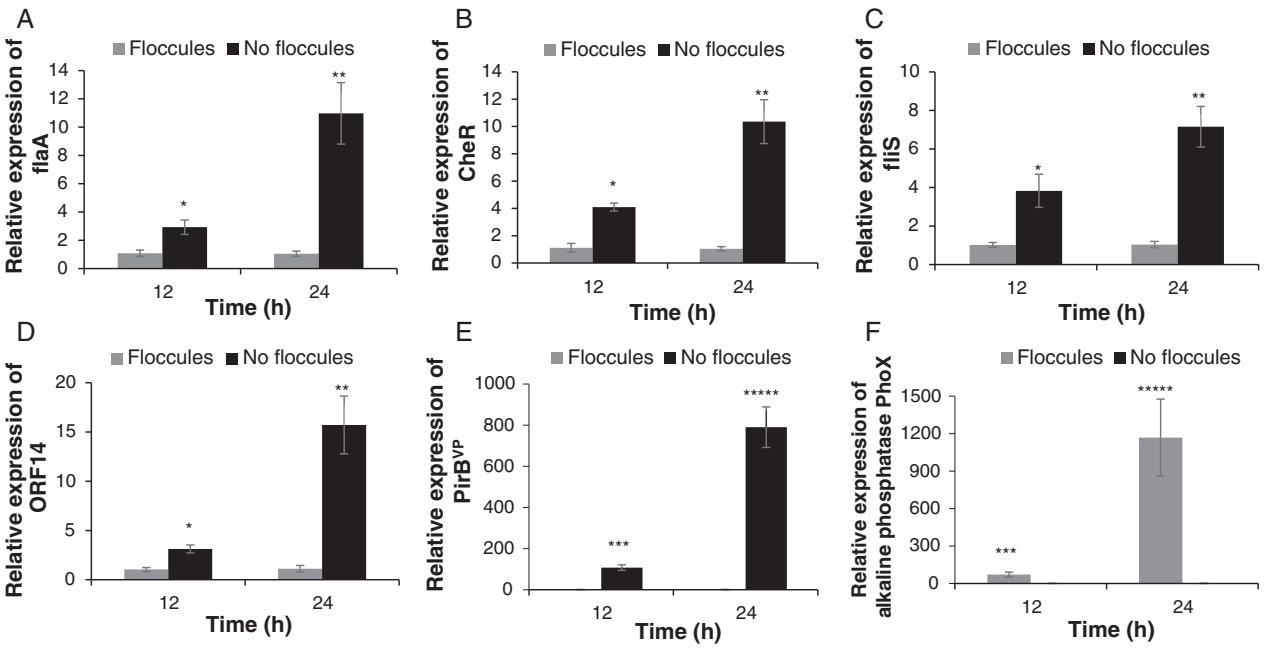

Fig. 5. Floccules formation associated with *ALP PhoX* gene expression attenuates the expression of flagella-related motility genes and virulent AHPND plasmid genes in *Vibrio parahaemolyticus* M0904 strain.
Expression of flagella-related motility genes: A, *flaA* (polar flagellin); B, *flis* (polar flagellin specific chaperone); C, *cheR* (chemotaxis protein). Virulent AHPND plasmid genes: D, *ORF14*; E, $PirB^{VP}$. Genes responsible for floccule formation: F, *ALP PhoX* from *V. parahaemolyticus* M0904 strain from M0904/110 (floccule) or M0904/120 (no floccule).
Samples from both culture conditions were collected for gene expression assay after 12 and 24 h. For the flagella-related motility genes and virulent AHPND plasmid genes, the expression in the floccules group (M0904/110) was set at 1. However, for *ALP PhoX* gene, the expression in the non-floccules group (M0904/120) was set at 1. The results are the mean ± standard error ($n = 3$) and are presented relative to *V. parahaemolyticus toxR* and *rpoA* mRNA. Asterisks represents significant difference between the *V. parahaemolyticus* M0904 culture with floccules (M0904/110) and no floccules (M0904/120).
*$p < 0.05$; **$p < 0.01$; ***$p < .001$; ****$p < 0.0001$; *****$p < 0.00001$.

and *ORF-14* (coding gene of plasmid) that mediates the virulence of *V. parahaemolyticus* in shrimp (Han *et al*., 2015; Sirikharin *et al*., 2015; Kumar *et al*., 2019b) was examined. Interestingly, the expression of virulent plasmid genes was significantly down-regulated in M0904/110 at 12 and 24 h as compared with M0904/120 (Fig. 5D,E). This observation is in line with the results on secreted proteins (mentioned above) and highlights that M0904/110 culture significantly decreases the transcription of virulence genes.

Considering that in altered environmental condition, *V. parahaemolyticus* produces floccules and secrete ALP PhoX protein (as shown in Fig. 3), the temporal expression of *ALP PhoX* gene in *V. parahaemolyticus* (M0904/110 or M0904/120) was investigated. As expected, the expression of *ALP PhoX* gene was significantly increased at 12 and 24 h in M0904/110, when compared with the M0904/120 (Fig. 5F). Taken together, these results imply that *V. parahaemolyticus* in lower speed shaking condition switch its phenotype, which in turn leads to decreased transcription of virulence-related genes and increased the expression of *ALP PhoX* gene.

AHPND V. parahaemolyticus *M0904 grown in lower shaking conditions displays reduced toxicity towards brine shrimp larvae*

Next, the *in vivo* virulence of *V. parahaemolyticus* was investigated using gnotobiotic brine shrimp larvae, used as a model for studying crustacean host-pathogen interaction (Baruah *et al*., 2015, 2017). At first, the toxicity of M0904/110 or M0904/120 towards brine shrimp larvae was examined. The results showed that larvae that were challenged with M0904/110 exhibited significantly increased survival compared with the larvae challenged with M0904/120 (Fig. 6A). Next, the toxicity of *V. parahaemolyticus* ECPs (VP_{AHPND} ECP) purified from either M0904/110 or M0904/120 cells was investigated. Interestingly, the results showed that toxicity towards *Artemia* of VP_{AHPND} ECP purified from M0904/110, decreased significantly when challenged with 1.3, 2.6, 3.9 and 5.2 μg 100 μl^{-1} as compared with VP_{AHPND} ECP purified from M0904/120 culture (Fig. 6B). Although, the toxicity of VP_{AHPND} ECP purified from *V. parahaemolyticus* grown in either M0904/110 or M0904/120 was

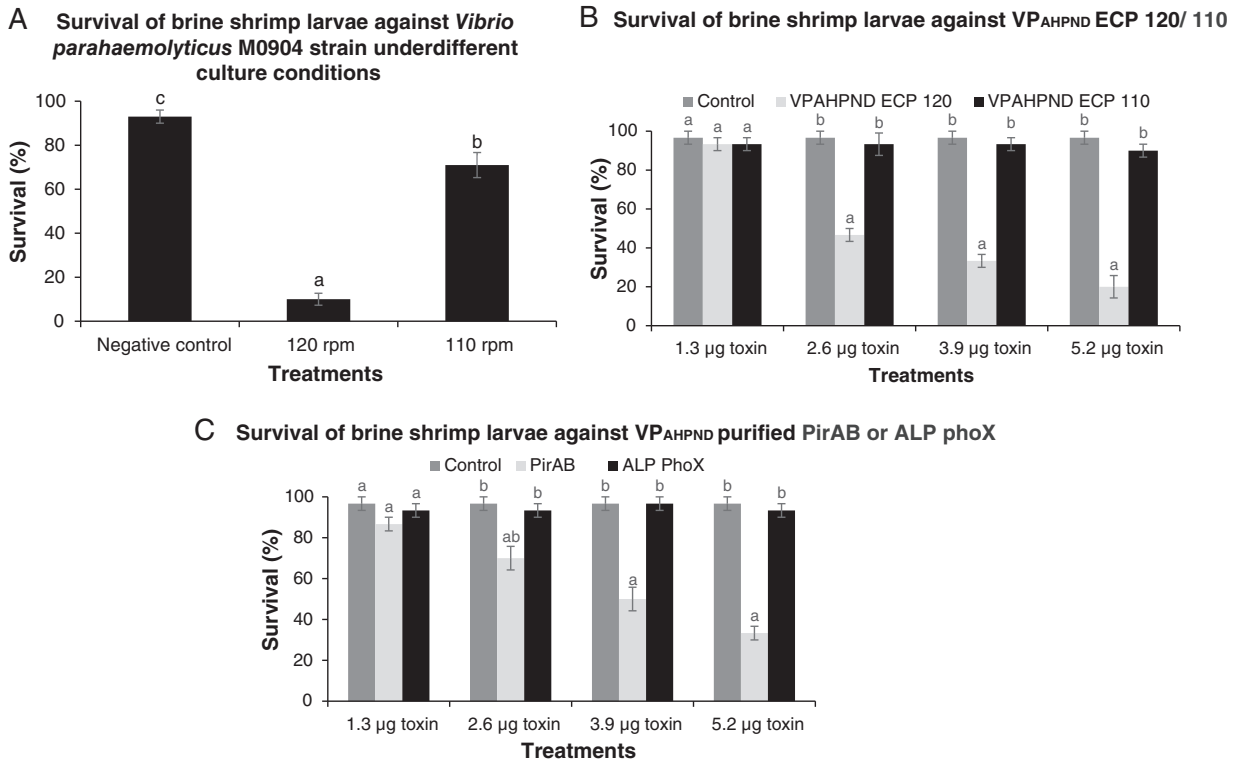

Fig. 6. The AHPND *Vibrio parahaemolyticus* grown in lower shaking condition reduces the toxicity of AHPND strain in brine shrimp larvae.
A. Survival (%) of brine shrimp larvae after 48 h of challenge with *V. parahaemolyticus* M0904 culture, M0904/120 and M0904/110. The larvae were challenged with *V. parahaemolyticus* at 10^7 cells ml^{-1} of rearing water. Non-challenged larvae were served as a negative control. Error bars represent the standard error of five replicates; different letters indicate significant differences ($p < 0.001$).
B. Survival (%) of *brine shrimp* larvae after 60 h of challenge with VP_{AHPND} ECP, obtained from either M0904/120 (ECP 120) or M0904/110 (ECP 110) at the concentrations of 1.3, 1.95, 2.6 and 3.9 µg 100 $µl^{-1}$ of FASW. Non-challenged larvae served as a negative control. Error bars represent the standard error of three replicates; different letters indicate significant differences ($p < 0.001$).
C. Survival (%) of *brine shrimp* larvae after 60 h of challenge with VP_{AHPND} purified $PirA^{VP}$ and $PirB^{VP}$ toxins or ALP PhoX (ALP PhoX) at the concentrations of 1.3, 1.95, 2.6 and 3.9 µg 100 $µl^{-1}$ of FASW. The non-challenged larvae served as a negative control. Error bars represent the standard error of three replicates; different letters indicate significant differences ($p < 0.001$).

significantly different, it is important to assess the toxicity of pure ALP PhoX as compared with pure $PirA^{VP}$ and $PirB^{VP}$ toxins. However, apart from ALP PhoX or $PirA^{VP}$ and $PirB^{VP}$ toxins, *V. parahaemolyticus* may also secrete some other proteins or toxins that might contribute to the toxicity of ECP towards brine shrimp larvae (Sirikharin *et al*., 2015). To do this, the purified ALP PhoX or $PirA^{VP}$ and $PirB^{VP}$ toxins, respectively, from M0904/110 or M0904/120 was used to challenge brine shrimp larvae at the concentrations of 1.3, 2.6, 3.9 and 5.2 µg 100 $µl^{-1}$. In agreement with the previous VP_{AHPND} ECP survival results, the results showed that brine shrimp larvae exposed to varying concentration of pure ALP PhoX enzyme has significantly increased survival percentage when compared with $PirA^{VP}$ and $PirB^{VP}$ toxins (Fig. 6C). Taking these results together, our *in vivo* assays confirm that shaking speed indeed plays an essential role in mediating virulence of *V. parahaemolyticus* towards brine shrimp larvae.

Floccule formation decreases the toxicity of AHPND V. parahaemolyticus *M0904 strain in* Macrobrachium rosenbergii *larvae*

The differential virulence of M0904/110 or M0904/120 cells was verified in another shrimp species, namely, freshwater shrimp, *Macrobrachium rosenbergii*. The results showed that survival of *Macrobrachium* larvae exposed to M0904/110 cells was significantly higher at 12, 24, 36 and 48 h post-challenge compared with larvae challenged with M0904/120 cells (Fig. S3) which is consistent with the results obtained with the brine shrimp larvae.

Discussion

The study describes that the AHPND-causing *V. parahaemolyticus* M0904 bacterial strain in response to low shaking conditions switches its phenotype to a state that helps the bacteria to produce levan-containing

biofilm and develops tolerance against antimicrobial agents, presumably allowing the bacterium to adapt to the altered environmental conditions (Singh *et al*., 2017). This altered physiological status not only led to a significant decrease in the secretion of virulence-related proteins ($PirA^{VP}$/$PirB^{VP}$) but also decreases the virulence of *V. parahaemolyticus* to shrimp.

In shaking flask, a number of parameters determine shear stress. Power input and/or shaking frequency, medium volume/flask volume ratio and medium viscosity contribute to the establishment of a certain amount of shear stress (Yayanos *et al*., 1981; Kato *et al*., 1998; Crump *et al*., 2004; Crabbé *et al*., 2008; Giese *et al*., 2014; Mancilla *et al*., 2015; Dingemans *et al*., 2016). Many bacteria modulate their behaviour in function of shear stress as imposed by flask shaking conditions. In *Pseudomonas aeruginosa*, low shear stress leads to the formation of self-aggregating biofilm. At the same time, genes involved in motility, type VI secretion, multidrug efflux were downregulated, while many other genes are upregulated (Poelwijk *et al*., 2006; De Visser and Krug, 2014; Tadrowski *et al*., 2018). We propose that a critically low shaking frequency favours the production of self-aggregating biofilm in M0904 like it was described in *Pseudomonas*. These self-aggregating biofilms present themselves as macroscopically visible flocs in shaking flask.

Levan, a major fructose polymer produced by Gram-negative bacteria, plays a crucial role in the formation of EPS matrix and biofilm (Franken *et al*., 2013), and the observed enhanced production of levan by *V. parahaemolyticus* could be an efficient adaptive strategy to promote EPS formation and biofilm production during low fluid shear growth conditions (M0904/110). These observations therefore strongly suggests that *V. parahaemolyticus* during low fluid shear growth condition (M0904/110) might not live as dispersed cells but instead accumulate at interfaces to form clusters or aggregates and switch to biofilm mode of life (Freeman *et al*., 1989; Phuoc *et al*., 2009; Jayaraman, 2011; Sousa *et al*., 2011).

We further tested for the generality of the adaptive phenotypic response of *V. parahaemolyticus* to low fluid shear conditions by verifying antimicrobial resistance. *Pseudomonas* develops biofilms at the air–liquid interface when grown under low fluid shear or static culture condition, protecting the bacterium from antibiotics (Rainey and Travisano, 1998; Balaban *et al*., 2004; Allegrucci and Sauer, 2007; Chantratita *et al*., 2007; Velázquez-Hernández *et al*., 2009; Dingemans *et al*., 2016). In this setting, oxygen is more limited and *Pseudomonas* outcompete others in the culture by increasing their access to oxygen (Spiers *et al*., 2002; Hansen *et al*., 2007). In parallel with the *Pseudomonas* experiment, it was observed that *V. parahaemolyticus* M0904 grown in low fluid shear condition (M0904/110) displays resistance to antibiotics (Fig. S1, Table 1). This suggests that resistance of *V. parahaemolyticus* to antimicrobial agents is a consequence of elevated biofilm production (Dharmaprakash and Thomas, 2016), which could possibly be mediated by shear stress-induced levan production (Guo and Gross, 2014; Kemper *et al*., 2014), although other mechanisms like enzyme-related resistance, genetic adaptation or limited diffusion of antimicrobial agents through the biofilm matrix are potentially possible (Vilain *et al*., 2002; Hall and Mah, 2017; Singh *et al*., 2017).

Other genes, associated with phenotypic changes, also displayed altered expression (Kent *et al*., 2018). *V. parahaemolyticus* modified the expression of biofilm associated genes, that is, flagella-related motility, Pir toxin, AHPND plasmid and *ALP PhoX* genes. The change in flow characteristic in a culture flask apparently leads to decreased expression of the virulence-related genes, while the expression of *ALP PhoX* gene was increased (Fig. 5). It has been described that in aggregating bacterial cells, the expression of flagella-related motility genes and other virulent genes is inhibited (Guttenplan and Kearns, 2013; Shikuma *et al*., 2013; Zhang *et al*., 2018). However, the first step in a transcriptional response is to convert the signals from the environment into transcriptional change, leading to the production of new proteins. Here low shear stress conditions modified strongly the protein secretome with ALP PhoX becoming a dominant member of it, while the production of $PirA^{VP}$ and $PirB^{VP}$ toxins was halted. (Fig. 3). As a major phosphatase enzyme in prokaryotes, the ALP are encoded by *ALP PhoX* gene and exported from the bacterial cytoplasm to the extracellular environment during biofilm mode of life (Golovastov *et al*., 2000; Liu *et al*., 2016; Favre *et al*., 2018). The phosphate starvation condition resulting in higher ALP activity in biofilms is probably due to mass transfer limitation in the polymer matrix (Vilain *et al*., 2002). ALP is involved in dephosphorylation reaction in many types of molecules (nucleotides, proteins and alkaloides) and enhances the bacterial colonization on artificial surfaces (Grant, 1979; Gross *et al*., 2001; Nalini *et al*., 2015), and this is consistent with higher ALP PhoX production in *V. parahaemolyticus* culture (M0904/110) potentially sustaining biofilm formation. In addition, ALP has also been shown to possess phosphodiesterase (PDE), and increased activity of PDE was shown to cause hyper-formation of biofilm in *Staphylococcus aureus* (Wu *et al*., 2007; Kageyama *et al*., 2011; Kalivoda *et al*., 2013). In fact, the pathogenic *Enterococcus faecalis* was reported to sense the outer environment and induce remodelling of cellular phospholipids content leading to enhanced antibiotic resistance and virulence of

the bacterium (Khan *et al*., 2019). It is therefore possible that ALP PhoX produced by this *V. parahaemolyticus* AHPND strain under low fluid shear growth condition (M0904/110) is a driving force to maintain a sufficiently high inorganic phosphorus supply in the extracellular microenvironment to promote biofilm formation and increased antimicrobial resistance (Nalini *et al*., 2015; Danikowski and Cheng, 2018). Although, in other bacterial species, ALP has been reported to play an important role in biofilm formation (Golovastov *et al*., 2000; Vilain *et al*., 2002; Liu *et al*., 2016; Favre *et al*., 2018), this is the first descriptive study illustrating that by switching to the biofilm floc-forming phenotype, *V. parahaemolyticus* changes the secretome pattern, over-expressing ALP PhoX enzyme.

The halophilic aquatic bacterium *V. parahaemolyticus* and especially AHPND-causing strains, such as M0904, are a major cause of infectious disease and mortality in wild and cultured shrimps (Lee *et al*., 2015; Li *et al*., 2017). The AHPND M0904 strain, harbouring the pVA1 plasmid (63–70 kb), expresses deadly toxins, that is, $PirA^{VP}$ (13 kDa) and $PirB^{VP}$ (50 kDa) that damages the shrimp tissue, primarily the hepatopancreas, and causes AHPND, with significant production losses to the shrimp farming industry (Tran *et al*., 2013; Han *et al*., 2015; Lee *et al*., 2015; Sirikharin *et al*., 2015; Li *et al*., 2017; Kumar *et al*., 2019a). However, this study does demonstrate how low fluid shear condition can rapidly downregulate virulence-related genes including Pir toxins, while upregulating *ALP PhoX* gene. Interestingly, the *in vivo* studies have shown that low fluid shear condition strongly reduced the virulence of *V. parahaemolyticus* to the host model species, that is, brine shrimp (*Artemia franciscana*) and freshwater prawn (*M. rosenbergii*) (Figs 6 and S3), supporting that phenotype switching does modulate virulence *in vivo*.

Together, the *in vitro* and *in vivo* observations allow to formulate a working hypothesis for the importance of biofilm formation in AHPND in shrimp. Certain environmental conditions, like low shear stress, will stimulate M0904 to form biofilm, a phenomenon very regularly observed in an aquaculture setting. This phenotype displays higher resistance to antimicrobial agents (as verified here by a higher antibiotic resistance). Such biofilms might become a reservoir of M0904 cells from which they can recolonize the aqueous environment in the form of planktonic cells. The latter cells might infect the host, allowing to produce $PirA^{VP}$/$PirB^{VP}$ toxins, and might cause AHPND. Hence it would be of interest in the future to determine whether or not one or both phenotypic forms are colonizing the hepatopancreas in shrimp and whether this is associated with toxin production. The expression of $PirA^{VP}$/$PirB^{VP}$ toxins or ALF PhoX might be used as phenotypic markers in such a study. These phenotypic markers might also be used to study environmental cues that modulate the phenotypic switch both in the aqueous environment as in the host. Such studies might enhance significantly our understanding of the behaviour of AHPND *V. parahaemolyticus* in aquaculture settings and open the possibility to combat AHPND not only by trying to eliminate the *Vibrio* from the system (which has been tried by antibiotics, a mode of operation which might only eliminate the planktonic form, based on our *in vitro* observations) but rather to steer the phenotypic switch.

Materials and methods

Bacterial strains and growth conditions

Total two bacterial strains were used in the study: *V. parahaemolyticus* M0904 (AHPND strains) (LMG P-31518) and *Aeromonas hydrophila* LVS3 (LMG 22148) (Defoirdt *et al*., 2006; Kumar *et al*., 2018). LVS3 (autoclaved) were used as feed for *Artemia* larvae and M0904 were used for toxin and enzyme production for the challenge assay. The stock culture of M0904 was streaked onto marine agar (MA) plates (Carl Roth, Leuven, Belgium) to obtain pure colonies. A single colony was inoculated into marine broth (MB) (Carl Roth), incubated overnight at 28°C under constant agitation (120 rpm), and the stock culture was prepared in 40% glycerol and stored at −80°C. The LVS3 culture was collected from the Laboratory of Aquaculture and *Artemia* Reference Center, Ghent University, Belgium. The strain was streaked onto MA plates (Carl Roth), afterwards single colony was inoculated in MB (Carl Roth), and the stock culture was prepared in a similar manner.

Detection of biofilm formation in AHPND V. parahaemolyticus *culture*

The biofilm formation and quantification were evaluated on the walls and bottom of the culture tubes as described by Henthorn and colleagues (1988), Hassan and colleagues (2011) and Danikowski and Cheng (2018) with slight modifications. Briefly, 50 µl of *V. parahaemolyticus* M0904 strain stock culture was inoculated into 20 ml of sterile MB in 50 ml Erlenmeyer flasks and grown overnight at 28°C under constant agitation (120 rpm). The overnight culture was diluted with fresh MB to an OD_{550nm} of 0.1 and further incubated overnight at 28°C with either 110 rpm (M0904/110) or 120 rpm (M0904/120) constant agitation. After 24 h incubation, the tubes were decanted and rinsed with PBS followed by staining with 0.1% (1 g l^{-1}) crystal violet at room temperature for 10 min. Excess stain was rinsed with deionized water, and the tubes were left to air dry in an inverted position. The crystal violet was extracted from each tube

by adding 33% acetic acid. Subsequently, 100 μl of extractions were transferred to 96-well tissue culture plate and absorbance was measured at 570 nm wavelength using infinite 200 Tecan plate reader (Tecan, Männedorf, Switzerland). The assay was performed in triplicate and is representative of two independent experiments.

Analysis of V. parahaemolyticus *cells cultured under different conditions*

Light and fluorescence microscopies. The *V. parahaemolyticus* M0904 strain culture, M0904/110 or M0904/120, was observed by using light and fluorescence microscope to observe the changes at cellular level. At first, 20 μl of bacterial suspension of either M0904/110 or M0904/120 was put onto a clean glass slide. Then a cover glass was placed over the sample, and excess liquid was removed by gently pressing the cover glass. The samples were observed under the light microscope (Zeiss Axioskop 2 plus, Carl Zeiss, Jena, Germany) at 10×, 40×, 36× and 100× magnification to detect the floccules formation by the bacterial strain. Later, the bacterial samples were stained with Calcofluor white stain (Sigma-Aldrich, St. Louis, MO) to detect the extracellular polysaccharides in the floccules produced by *V. parahaemolyticus* M0904 strain through a fluorescence microscope (Zeiss Axioskop 2 plus, Carl Zeiss). Briefly, 20 μl of bacterial suspension (M0904/110 or M0904/120) was put onto a clean glass slide. Afterwards, one drop of Calcofluor white stain and one drop of 10% potassium hydroxide were added to the samples (according to the manufacturer instructions). The samples were covered with cover glass and incubated for 1 min at room temperature. Subsequently, the slides were examined under a fluorescence microscope with the excitation of band pass (BP) 365/12, beam splitter FT 395 and emission long pass 397 at 10×, 40×, 36× and 100× magnification.

Flow cytometry. The *V. parahaemolyticus* M0904 strain culture, M0904/110 or M0904/120, was diluted to 5×10^9 cells ml^{-1} with sterile MB using spectrophotometer (Genesys 20, Thermo Spectronic). Afterwards, 1 ml of bacterial suspension was transferred to 2 ml sterile eppendorf tubes and centrifuged for 10 min at 8000*g* in room temperature. The bacterial cells were collected and resuspended in 10 ml Tris-buffered saline (0.13 M NaCl and 10 mM Tris hydrochloride, pH 7.4). Later, 250 μl of bacterial cells in Tris-buffered saline was transferred to 2 ml sterile eppendorf tubes and 1 μl of FITC–lectin was added (seven different types of lectins were used with different glycan specificities, Table S2). The bacterial cell and lectin mixture were then transferred to 96-well plate and to facilitate the binding of FITC–lectins to the bacteria cells, the plates were incubated for 30 min in dark at room temperature.

Subsequently, the samples were analyzed with a CytoFLEX flow cytometer system (Beckman Coulter's Life sciences, France) equipped with a 37 m (pore size) filter, a 75 μm (pore size) orifice and a 0.3 neutral density filter and photomultiplier tube set at 500 V. The calibration and standardization of the flow cytometer were done in accordance with manufacturer specifications. The fluorescent microbeads were used as standards for fluorescence, and volume and green fluorescence were measured at 525 nm (FITC) and 488 nm [forward scatter (FSC)]. The flow cytometer was set as follows: gain FSC-106, gain FITC-113 and speed-4 (implying an event rate never exceeding 1000 events per second). Counts were recorded as logarithmic signals and were triggered on the green fluorescence channel. Data were processed with CytExpert software (Beckman Coulter's Life sciences, France), using electronic gaining to separate the desired events. Presentation of the data as FITC/count or FSC/count histogram plot allowed for an optimal distinction between FITC-lectins labelled bacteria cells and instrument noise or sample background (Hammes and Egli, 2010; Frossard *et al*., 2016).

MACR plate method. The MACR plate method was used out to determine the production of extracellular slime by *V. parahaemolyticus* M0904 strain following the procedure as described by Freeman and colleagues (1989) and Phuoc and colleagues (2009) with slight modifications. Briefly, the *V. parahaemolyticus* M0904 culture were incubated for 24 h at 28°C in 20 ml MB with constant agitation at either 110 rpm (M0904/110) or 120 rpm (M0904/120). Subsequently, the broth was discarded, and cells attached to the bottom of the Erlenmeyer were collected after adding and mixing with 5 ml of filtered autoclaved seawater (FASW). The bacterial suspension in FASW was streaked onto MACR plates (37.4 g MB, 50 g sucrose, 15 g agar and 0.8 g Congo red). The Congo red was prepared as a stock solution, autoclaved and then added to the culture medium when it had cooled to 55°C. After inoculation, the plates were incubated for 24 h at 28°C. The bacterial strains that produce extracellular slime develop different colour colonies in MACR plates (Freeman *et al*., 1989; Mariana *et al*., 2009). The assay was performed in triplicate and is representative of two independent experiments.

Antibiotic susceptibility test

The antibiotic susceptibility test for *V. parahaemolyticus* M0904 cells, M0904/110 or M0904/120 was determined by the *in vitro* agar diffusion method (Balouiri *et al*., 2016;

Zidour *et al*., 2017) using antibiotic discs (Oxoid, Basingstoke). For this study, five different antibiotic discs (6 mm diameter) were used per quintuplicate [chloramphenicol (30 μg), tetracycline (30 μg), ampicillin (25 U), kanamycin (30 μg) and rifampicin (30 μg)]. Briefly, the overnight grown *V. parahaemolyticus* M0904 strain culture (M0904/110 or M0904/120) was diluted to 10^6 cells ml^{-1} with sterile MB using spectrophotometer (Genesys 20, Thermo Spectronic). Subsequently, the bacterial suspensions (100 μl) were spread onto MA plates using sterile spreader, and five different antibiotic discs were placed on each agar plates with a dispenser. Later, the agar plates were covered with parafilm tape and were incubated for 24–48 h at 28°C. Diameters of inhibition halos surrounding the discs were measured and expressed in millimeters. Results were interpreted as sensitive, intermediate, or resistant, following the guidelines of the Clinical and Laboratory Standards Institute (NCCLS, 2002; CLSI, 2015). The assay was performed in quintuplicate and is representative of two independent experiments.

Purification of V. parahaemolyticus *ECP (VP_{AHPND} ECP)*

In total, two separate tests were performed. Briefly, the *V. parahaemolyticus* M0904 strain was grown overnight at 28°C in 20 ml MB in 50 ml Erlenmeyer with constant agitation at either 110 rpm (M0904/110) or 120 rpm (M0904/120). The overnight grown bacterial suspension was centrifuged for 15 min at 3500*g*. The supernatant was collected and filtered with a 0.2-μm sieve to obtain cell-free supernatant (CFS) of *V. parahaemolyticus*. The CFS of *V. parahaemolyticus* was then concentrated and dialyzed with PBS with 10 kDa amicon® ultra-15 centrifugal filters (Merck Millipore, Burlington, MA) (Kumar *et al*., 2019b). The concentrated ECP (VP_{AHPND} ECP) was collected and immediately preserved at −80°C for further analysis.

Mass spectrometry-based analysis of $PirA^{VP}$ and $PirB^{VP}$ toxins and ALP PhoX from VP_{AHPND} ECP

To identify the presumptive proteins produced by *V. parahaemolyticus* AHPND strain from different culture conditions (M0904/110 or M0904/120), the concentrated VP_{AHPND} ECP (ECP 110 or ECP 120) samples were combined with loading buffer, vortexed, heated for 5 min at 95°C and separated by SDS-PAGE on 4%–20% polyacrylamide gel (BioRad, Temse, Belgium), with each lane receiving equivalent volume (10 μl) of protein. The gels were stained with Coomassie Biosafe (BioRad), and the signals were detected by a ChemiDoc MP imaging system (BioRad). The protein concentration was determined by the Bradford method (Bradford, 1976) using BSA as standard. The possible candidate bands of $PirA^{VP}$ and $PirB^{VP}$ toxins and ALP PhoX on Coomassie stained SDS-PAGE gels were excised using a clean scalpel (preferentially under the laminar flow to avoid the keratin contamination), and the gel pieces (with a clean pincet) were transferred into sterile eppendorf tubes. The gel pieces were rinsed twice with 500 μl of sterile distilled water and stored at −20°C until further processing by liquid chromatography–tandem mass spectrometry (LC–MS/MS) analysis.

To prepare the samples for LC–MS/MS, the gel pieces were washed consecutively with water, acetonitrile (ACN) in water (50/50, vol/vol) and ACN and were then dried completely using a rotary evaporator. The dried gel bands were rehydrated with 15 μl of a trypsin-containing solution (5 ng μl^{-1} in 50 mM ammonium bicarbonate) and after swelling of the gel pieces 50 mM ammonium bicarbonate was added until the bands were completely submerged. The samples were incubated overnight at 37°C for trypsin digestion and elution of the resulting peptides from the gel. Next day, formic acid was added to the eluted peptides to deactivate trypsin, and the peptides were dried completely in a rotary evaporator. For LC–MS/MS analysis, the dried peptide samples were dissolved in 20 μl loading buffer [0.1% trifluoroacetic acid (TFA) in water/ACN, 2/98 (vol/vol)], and half of each sample was injected on a tandem configurated Ultimate 3000 RSLC nanoLC (Thermo Fisher Scientific, Dreieich, Germany) in-line connected to an LTQ-Orbitrap Elite (Thermo Fisher Scientific) equipped with a pneu-Nimbus dual ion source (Phoenix S&T) and a Butterfly nano-LC column oven (Phoenix S&T) to keep the column temperature constant at 50°C. The sample mixture was first loaded on a trapping column (made in-house, 100 μm I.D. × 20 mm length, 5 μm beads C18 Reprosil-HD, Dr. Maisch) and after flushing from the trapping column, the sample was separated on a reverse-phase analytical column (made in-house, 75 μm I.D. × 200 mm length, 1.9 μm beads C18 Reprosil-HD, Dr. Maisch). Peptides were separated with a nonlinear 90 min gradient from 98% solvent A (0.1% formic acid in water) to 56% solvent B [0.1% formic acid in water/ACN 20:80 (vol/vol)], all at a constant flow rate of 250 nl min^{-1} followed by a 5 min wash reaching 99% solvent B.

The mass spectrometer was operated in data-dependent, positive ionization mode, automatically switching between MS and MS/MS acquisition for the 20 most abundant peaks in a given MS spectrum. The source voltage was set at 3 kV, and the capillary temperature was 275°C. In the LTQ-Orbitrap Elite, full-scan MS spectra were acquired in the Orbitrap (*m*/*z* 300–2000, AGC target 3×10^6 ions, maximum ion injection time 100 ms) with a resolution of 60,000 (at 400 *m*/*z*). The 20 most intense ions fulfilling pre-defined selection criteria

(automatic gain control [AGC] target 5×10^3 ions, maximum ion injection time 20 ms, exclusion of unassigned and singly charged precursors, dynamic exclusion time 20 s) were then isolated in the linear ion trap and fragmented in the high-pressure cell of the ion trap. The collision induced dissociation energy was set to 35 V and the polydimethylcyclosiloxane background ion at 445.120028 Da was used for internal calibration (lock mass).

Data analysis was performed with MaxQuant (version 1.6.2.6) using the Andromeda search engine with default search settings including a false discovery rate set at 1% on the peptide spectrum match, peptide and protein level. Spectra were searched against the proteins of *V. parahaemolyticus* strain 20130626002S01 in the database (CP020076) (containing 5004 *Vibrio* protein sequences) supplemented with the sequences of the $PirA^{VP}$ (gil922,664,586) and $PirB^{VP}$ toxins (gil 922,664,588). The mass tolerance for precursor and fragment ions was set to 4.5 and 20 ppm, respectively, during the main search. Enzyme specificity was set as C-terminal to arginine and lysine, also allowing cleavage at proline bonds with a maximum of two missed cleavages. Variable modifications were set to oxidation of methionine residues, propionamidation of cysteine residues and acetylation of protein N-termini. Only proteins with at least one unique or razor peptide were selected. A minimum ratio count of two unique or razor peptides was required for quantification. The resulting protein lists from the MaxQuant protein groups file were sorted on descending iBAQ ratio, revealing $PirA^{VP}$, $PirB^{VP}$ and PhoX as most abundant protein in their respective protein bands. The identified peptides of $PirA^{VP}$ and $PirB^{VP}$ toxins were mapped on the corresponding protein sequence.

ALP activity assay

In total, three separate tests were carried out to determine the phosphate-solubilizing activity of *V. parahaemolyticus* AHPND strain in Pikovskayas agar (1.5%) under different culture conditions. Briefly, after solidification of Pikovskayas agar, around 10 mm well diameter was cut out aseptically under laminar flow. In the first experiment, the well was filled with overnight *V. parahaemolyticus* M0904 strain cultured in 20 ml MB under constant agitation in 110 or 120 rpm. In the second test, the agar plate wells were filled with *V. parahaemolyticus* concentrated ECP with ALP PhoX or $PirA^{VP}$ and $PirB^{VP}$ toxins. Afterwards, the agar plates were incubated at 30°C for a period of 48–72 h and observation was made for the appearance of a clear zone around the well which indicates the solubilization of phosphate.

In the third experiment, the putative phosphate-solubilizing activity of purified ALP PhoX as compared with $PirA^{VP}$ and $PirB^{VP}$ toxins was determined. At first, the respective bands of interest were excised from polyacrylamide gels and placed in eppendorf tubes. The tubes were filled with 1 ml elution buffer (50 mM Tris–HCl, 150 mM NaCl and 0.1 mM EDTA; pH 7.5), and the gel pieces were crushed using sterile microfuge pestle and incubated overnight on shaker at 30°C. Subsequently, the eppendorf tubes were centrifuged at 10 000*g* for 10 min, and the supernatant were collected in a new eppendorf tubes. The supernatant was electrophoresed in 4%–20% SDS-PAGE gel (BioRad), stained with Coomassie Biosafe (BioRad Laboratories) and then visualized by a ChemiDoc MP imaging system (BioRad) to verify the presence of purified proteins. Later, the wells of Pikovskayas agar plates were filled with either purified ALP PhoX or $PirA^{VP}$ and $PirB^{VP}$ toxins and the appearance of clear zone around the well which indicates the phosphate solubilization was observed after 48–72 h as described above.

Polymerase chain reaction confirmation for the presence of AHPND plasmid in V. parahaemolyticus *cultures*

The *V. parahaemolyticus* M0904 strain culture, M0904/110 or M0904/120, was confirmed to harbour the AHPND plasmid by polymerase chain reaction (PCR) using AP3 primers (Table S3). The AP3-based PCR fragment was not present in non-AHPND *V. parahaemolyticus* (Fig. S4) (Sirikharin *et al*., 2014; Suong *et al*., 2017).

RNA extraction and reverse transcription

The *V. parahaemolyticus* M0904 strain was grown overnight in triplicate in 20 ml sterile MB at either 110 rpm (M0904/110) or 120 rpm (M0904/120). Cells were harvested after 12 and 24 h of incubation, and total RNA was extracted with Qiagen RNeasy Plus Mini Kit (Cat No. 74136) from the bacterial samples in triplicate according to the manufacturer's instructions. The RNA quality and quantity were measured on NanoDrop spectrophotometer (Thermo Fisher Scientific), and RNA samples with A260/A280 ratios > 2.0 and A260/A230 ratios > 1.5 were used for the analysis. The RNA integrity was checked by agarose gel electrophoresis, and the RNA samples were stored at −80°C for subsequent use.

Reverse transcription was done with the RevertAid™ H Minus First Strand Complementary DNA (cDNA) Synthesis Kit (Thermo Fisher Scientific according to the manufacturer's guidelines. Briefly, 1 μg of total RNA and 1 μl of random hexamer primer solution were mixed first. Then, 8 μl of reaction mixture containing 4 μl of 5× reaction buffer (0.25 mol^{-1} Tris–HCl pH 8.3, 0.25 mol^{-1} $MgCl_2$, 0.05 mol^{-1} DTT), 2 μl of 0.01 mol^{-1} dNTP mix, 20 units of ribonuclease inhibitor, 200 units of RevertAid™ H

minus M-MuLV reverse transcriptase was added. The reaction mixture was incubated for 5 min at 25°C followed by 60 min at 42°C. The reaction was terminated by heating at 70°C for 5 min and then cooled to 4°C. cDNA samples were checked by PCR and stored at −20°C for further use.

Quantitative real-time PCR analysis

The expression of three flagella-related motility genes, that is, regulators, structural and chemotaxis genes, two VP_{AHPND} plasmid-related virulent genes, that is, toxin and coding genes of virulent plasmid, and one *ALP PhoX* gene associated with floccules formation were measured by quantitative real-time PCR (RT-qPCR) with a pair of specific primers using StepOnePlus RT-PCR systems (Applied Biosystems) (Table S4). The Ct values from the two reference genes *rpoA* (RNA polymerase A submit) and *toxR* mRNA, used as the internal control, were subjected to geomean, and expression of the genes was calculated relative to the *rpoA* and *toxR* mRNA levels. The amplification was performed in a total volume of 20 μl, containing 10 μl of 2× Maxima SYBR Green/ROX qPCR Master Mix (Thermo Fisher Scientific), 1 μl of cDNA (50 ng), 8 μl of nuclease free water and 0.5 μl of each specific primer. Master mixes were prepared for each biological replicate of the sample in triplicate, and RT-qPCR for target and reference genes was performed with a four-step amplification protocol: initial denaturation (10 min at 95°C); 40 cycles of amplification and quantification (15 s at 95°C, 30 s at 60°C and 30 s at 72°C); melting curve (55–95°C) with a heating rate of 0.10°C s^{-1} and a continuous fluorescence measurement) and cooling (4°C). A negative control reaction was included for each primer set by omitting template cDNA. The comparative cycle threshold method ($2^{-\Delta\Delta Ct}$ method) following Livak and Schmittgen (2001) was used to analyse the expression level of the target genes and verified by Pfaffl relative standard curve method (Pfaffl, 2002). The log-transformed $2^{-\Delta\Delta CT}$ values were subjected to a *t* test, and the *p* values smaller than 0.05 were considered statistically significant.

Axenic brine shrimp hatching

The gnotobiotic brine shrimp larvae were produced by hatching high-quality cysts axenically (germ-free) following decapsulation and hatching procedures as described by Baruah and colleagues (2014). Briefly, 200 mg of *A. franciscana* cysts (EG® type, batch 21452, INVE Aquaculture, Dendermonde, Belgium) was hydrated in 18 ml of distilled water for 1 h. Sterile cysts and larvae were obtained via decapsulation using 660 μl NaOH (32%) and 10 ml NaOCl (50%). During the reaction, 0.2 μm filtered aeration was provided. All manipulation was carried out under a laminar flow hood, and all tools were sterilized. The decapsulation was stopped after 2 min by adding 10 ml of $Na_2S_2O_3$ at 10 g l^{-1}. The decapsulated cysts were washed with FASW containing 35 g l^{-1} of instant ocean® synthetic sea salt (Aquarium Systems, Sarrebourg, France). The cysts were resuspended in 50 ml tube containing 30 ml of FASW and hatched for 24 h on a rotor (6 rpm) at 28°C with a constant illumination of approximately 27 μE (m^2 $s)^{-1}$. After 28 h of incubation, hatched larvae at developmental stage instar II (mouth is opened to ingest particles) were collected, and the axenicity was verified by spread plating (100 ml) as well as by adding (500 μl) of the hatching water on MA and MB, respectively, followed by incubating at 28°C for 5 days (Baruah *et al*., 2012). Experiments started with non-axenic larvae were discarded.

Brine shrimp challenge assay

Using the gnotobiotic brine shrimp larvae, three separate experiments were performed to determine the toxicity of *V. parahaemolyticus* M0904 strain cultured under different conditions. The toxicity assays were performed according to the method developed by Kumar and colleagues (2018). In the first experiment, the hatched brine shrimp larvae (at developmental stage II) were collected and a group of 20 larvae was transferred to sterile 40 ml glass tubes containing 10 ml FASW. Subsequently, the brine shrimp larvae were challenged with pathogenic *V. parahaemolyticus* M0904 cells incubated under constant agitation at 120 rpm (M0904/120) or 110 rpm (M0904/110) at 10^7 cells ml^{-1} and fed with autoclaved LVS3. In our previous work, it was observed that $PirA^{VP}$ and $PirB^{VP}$ toxins are released extracellularly and that the presence of toxin in broth medium alone can cause AHPND aetiology and mortality in shrimps (Kumar *et al*., 2019a; 2019b). Hence after challenge with bacterial cultures, that is, M0904/120 (no flocs) containing $PirA^{VP}$/$PirB^{VP}$ toxins or M0904/110 (flocculating) producing ALP PhoX, the brine shrimp glass tubes were incubated under the same conditions at 28°C. The survival of *Artemia* larvae was scored manually 48 h after the addition of pathogen. The non-challenged larvae were maintained as a negative control.

In the second experiment, a group of 10 brine shrimp larvae was collected and transferred to 2 ml sterile eppendorf tubes, containing 1 ml of FASW. Afterwards, the brine shrimp larvae were challenged with VP_{AHPND} ECP, obtained from either M0904/120 (ECP 120) or M0904/110 (ECP 110) at the concentration of 1.3, 1.95, 2.6 and 3.9 μg 100 μl^{-1} of FASW. The survival of larvae was scored 60 h after the addition of ECP. The non-challenged larvae were maintained as a negative control.

In the third experiment, a group of 10 brine shrimp larvae were counted and distributed into sterile 2 ml eppendorf tubes and then challenged with VP_{AHPND} purified $PirA^{VP}$ and $PirB^{VP}$ toxins or ALP PhoX at the concentrations of 1.3, 1.95, 2.6 and 3.9 μg 100 μl^{-1} of FASW, as described above in the lethality test. The non-challenged larvae were maintained as negative controls. The assays were performed in quintuplicate and are representative of two independent experiments.

M. rosenbergii *rearing system*

The experiments were carried out at the Laboratory of Aquaculture & *Artemia* Reference Center, Ghent University, Belgium, in a controlled temperature room. Acclimatized adult freshwater prawn (*M. rosenbergii*) obtained from the laboratory and maintained in four separate freshwater recirculation units were used as brooders. For each experiment, larvae from a single ovigerous female breeder were used. Matured female with fully ripe fertilized eggs (indicated by dark grey eggs) was transferred to the hatching tanks (30 l) containing brackish water (6 g l^{-1} salinity). Twenty-four hours after hatching, the larvae were collected and stocked in two separate brackish water (12 g l^{-1} salinity) recirculation units and fed with newly hatched axenic brine shrimp larvae. The broodstock management techniques were followed as previously described (Baruah *et al*., 2009; Nhan *et al*., 2010).

Macrobrachium *challenge assay*

The experiments were performed to determine the toxicity *V. parahaemolyticus* M0904 strain incubated under different culture conditions in *Macrobrachium* larvae (8 days old). Groups of 10 *Macrobrachium* larvae (8 days old) were collected and transferred to 150 ml glass tubes containing 100 ml of sterile brackish water (12 g l^{-1} salinity) (Rahman *et al*., 2004). Subsequently, the larvae were challenged with pathogenic *V. parahaemolyticus* M0904 cells incubated under constant agitation at 120 rpm (M0904/120) or 110 rpm (M0904/110) at 10^6 cells ml^{-1} (Kumar *et al*., 2018). The survival of larvae was scored at 12, 24, 36 and 48 h after the addition of pathogen. *Macrobrachium* larvae that were not challenged with *V. parahaemolyticus* served as a negative control. The assay was performed in quintuplicate and is representative of two independent experiments.

Statistical analysis

Survival data of brine shrimp larvae were arcsin transformed to satisfy normality and homoscedasticity requirements as necessary. The data were then subjected to one-way analysis of variances followed by Duncan's multiple range test using statistical software statistical package for the social sciences version 24.0. Probability values of ≤ 0.001 were considered significant. Gene expressions results were presented as fold expression relative to the geometrical mean of two internal control genes (*toxR* and *rpoA*). The expression level in the floccules forming group (M0904/110) was regarded as 1.0 and thereby the expression ratio of the non-floccule group (M0904/120) was expressed in relation to the control. Statistical analysis for the significant differences in the expression levels between the control and treatment was performed with single-tailed Student's *t* tests using the log-transformed data. Survival data of *M. rosenbergii* were subjected to logistic regression analysis using GenStat 16 (VSN International, Hemel Hempstead, UK) to determine significant differences between the control and treatment.

Acknowledgements

The authors thank Dr. Tyler Arbour, Center for Microbial Ecology and Technology (CMET), Ghent University for his support in microscopic analysis of bacterial samples. We would like to acknowledge the technical assistant provided by Brigitte Van Moffaert, Anita De Haese, Jorg De Smeyter and Phennapa promthale. Vikash Kumar is supported by Netaji Subhas International Doctoral Fellowship from Indian Council of Agricultural Research (ICAR), New Delhi. We highly acknowledge the Special Research Fund of Ghent University (BOF12/BAS/042) for procuring the chemiluminescence detection system. The flow cytometry results presented in this publication were carried out with infrastructure funded by EMBRC Belgium – FWO agreement 20151029-03 and Hercules agreement 20140910-03.

Author contributions

VK and PB conceived and designed the experiment. VK performed the experiments and drafted the figures and manuscript. VK, SR, DVH and FI made the laboratory analysis, statistics and interpreted data. Manuscript is reviewed and edited by VK, KB and PB. All the authors approved the final manuscript.

REFERENCES

Allegrucci, M., and Sauer, K. (2007) Characterization of colony morphology variants isolated from *Streptococcus pneumoniae* biofilms. *J Bacteriol* **189**: 2030–2038.

Balaban, N.Q., Merrin, J., Chait, R., Kowalik, L., and Leibler, S. (2004) Bacterial persistence as a phenotypic switch. *Science* **305**: 1622–1626.

Balouiri, M., Sadiki, M., and Ibnsouda, S.K. (2016) Methods for in vitro evaluating antimicrobial activity: A review. *J Pharm Anal* **6**: 71–79.

Baruah, K., Cam, D.T.V., Dierckens, K., Wille, M., Defoirdt, T., Sorgeloos, P., and Bossier, P. (2009) In vivo

effects of single or combined N-acyl homoserine lactone quorum sensing signals on the performance of *Macrobrachium rosenbergii* larvae. *Aquaculture* **288**: 233–238.

Baruah, K., Huy, T.T., Norouzitallab, P., Niu, Y., Gupta, S.K., De Schryver, P., and Bossier, P. (2015) Probing the protective mechanism of poly-ß-hydroxybutyrate against vibriosis by using gnotobiotic *Artemia franciscana* and *Vibrio campbellii* as host-pathogen model. *Sci Rep* **5**: 1–8.

Baruah, K., Norouzitallab, P., Linayati, L., Sorgeloos, P., and Bossier, P. (2014) Reactive oxygen species generated by a heat shock protein (Hsp) inducing product contributes to Hsp70 production and Hsp70-mediated protective immunity in *Artemia franciscana* against pathogenic vibrios. *Dev Comp Immunol* **46**: 470–479.

Baruah, K., Norouzitallab, P., Phong, H.P.P.D., Smagghe, G., and Bossier, P. (2017) Enhanced resistance against *Vibrio harveyi* infection by carvacrol and its association with the induction of heat shock protein 72 in gnotobiotic *Artemia franciscana*. *Cell Stress Chaperones* **22**: 377–387.

Baruah, K., Norouzitallab, P., Roberts, R.J., Sorgeloos, P., and Bossier, P. (2012) A novel heat-shock protein inducer triggers heat shock protein 70 production and protects *Artemia franciscana nauplii* against abiotic stressors. *Aquaculture* **334–337**: 152–158.

Bradford, M.M. (1976) A rapid and sensitive method for the quantitation of microgram quantities of protein utilizing the principle of protein-dye binding. *Anal Biochem* **72**: 248–254.

Campa-Córdova, A.I., León-Gallo, A.F., Romero-Maldonado, A., Ibarra-Serrano, A.C., Rosales-Mendoza, S., Hirono, I., and Angulo, C. (2017) Recombinant PirA-like toxin protects shrimp against challenge with *Vibrio parahaemolyticus*, the aetiological agent of acute hepatopancreatic necrosis disease. *J Fish Dis* **40**: 1725–1729.

Chantratita, N., Wuthiekanun, V., Boonbumrung, K., Tiyawisutsri, R., Vesaratchavest, M., Limmathurotsakul, D., *et al*. (2007) Biological relevance of colony morphology and phenotypic switching by *Burkholderia pseudomallei*. *J Bacteriol* **189**: 807–817.

CLSI. (2015) Performance standards for antimicrobial susceptibility testing; twenty-fifth informational supplement. In *CLSI document M100-S25*, Wayne, P. (ed). Wayne, Pennsylvania: Clinical and Laboratory Standards Institute.

Crabbé, A., De Boever, P., Van Houdt, R., Moors, H., Mergeay, M., and Cornelis, P. (2008) Use of the rotating wall vessel technology to study the effect of shear stress on growth behaviour of *Pseudomonas aeruginosa* PA01. *Environ Microbiol* **10**: 2098–2110.

Crump, B.C., Hopkinson, C.S., Sogin, M.L., and Hobbie, J.E. (2004) Microbial biogeography along an estuarine salinity gradient: combined influences of bacterial growth and residence time. *Appl Environ Microbiol* **70**: 1494–1505.

Danikowski, K.M., and Cheng, T. (2018) Alkaline phosphatase activity of *Staphylococcus aureus* grown in biofilm and suspension cultures. *Curr Microbiol* **75**: 1226–1230.

Defoirdt, T., Crab, R., Wood, T.K., Sorgeloos, P., Verstraete, W., and Bossier, P. (2006) Quorum sensing-disrupting brominated furanones protect the gnotobiotic brine shrimp *Artemia franciscana* from pathogenic *Vibrio harveyi*, *Vibrio campbellii*, and *Vibrio parahaemolyticus* isolates. *Appl Environ Microbiol* **72**: 6419–6423.

Dewanti, R., and Wong, A.L. (1995) Influence of culture conditions on biofilm formation by *Escherichia coli* 0157: H7. *Int J Food Microbiol* **26**: 147–164.

Dharmaprakash, A., and Thomas, S. (2016) Identification of biofilm-stage specific proteins associated with multidrug resistance and quorum sensing pathway in a pandemic strain of *Vibrio parahaemolyticus* isolated from India. *Int J Infect Dis* **45**: 45–46.

Dingemans, J., Monsieurs, P., Yu, S.-H., Crabbé, A., Förstner, K., Malfroot, A., *et al*. (2016) Effect of shear stress on *Pseudomonas aeruginosa* isolated from the cyctic fibrosis lung. *MBio* **7**: 1–16.

Dong, X., Bi, D., Wang, H., Zou, P., Xie, G., Wan, X., *et al*. (2017) pirABvp-bearing *Vibrio parahaemolyticus* and *Vibrio campbellii* pathogens isolated from the same AHPND-affected pond possess highly similar pathogenic plasmids. *Front Microbiol* **8**: 1–9.

Favre, L., Ortalo-Magné, A., Pichereaux, C., Gargaros, A., Burlet-Schiltz, O., Cotelle, V., and Culioli, G. (2018) Metabolome and proteome changes between biofilm and planktonic phenotypes of the marine bacterium *Pseudoalteromonas lipolytica* TC8. *Biofouling* **34**: 132–148.

Fonseca, A.P., and Sousa, J.C. (2007) Effect of shear stress on growth, adhesion and biofilm formation of *Pseudomonas aeruginosa* with antibiotic-induced morphological changes. *Int J Antimicrob Agents* **30**: 236–241.

Franken, J., Brandt, B.A., Tai, S.L., and Bauer, F.F. (2013) Biosynthesis of levan, a bacterial extracellular polysaccharide, in the yeast *Saccharomyces cerevisiae*. *PLoS One* **8**: 1–14.

Freeman, D.J., Falkiner, F.R., and Patrick, S. (1989) New method for detecting slime production by coagulase negative Staphylococci. *J Clin Pathol* **42**: 872–874.

Frossard, A., Hammes, F., and Gessner, M.O. (2016) Flow cytometric assessment of bacterial abundance in soils, sediments and sludge. *Front Microbiol* **7**: 1–8.

Giese, H., Klockner, W., Pena, C., Galindo, E., Lotter, S., Wetzel, K., *et al*. (2014) Effective shear rates in shake flasks. *Chem Eng Sci* **118**: 102–113.

Golovastov, V.V., Mikhaleva, N.I., Yu Kadyrova, L., and Nesmeyanova, M.A. (2000) The major phospholipid of *Escherichia coli*, phosphatidylethanolamine, is required for efficient production and secretion of alkaline phosphatase. *Biochemistry* **65**: 1097–1104.

Grant, W.D. (1979) Cell wall teichoic acid as a reserve phosphate source in *Bacillus subtilis*. *J Bacteriol* **137**: 35–43.

Gross, M., Cramton, S.E., Go, F., and Peschel, A. (2001) Key role of teichoic acid net charge in *Staphylococcus aureus* colonization of artificial surfaces. *Infect Immun* **69**: 3423–3426.

Guo, M., and Gross, C.A. (2014) Stress induced remodeling of the bacterial proteome. *Curr Biol* **24**: R424–R434.

Guttenplan, S.B., and Kearns, D.B. (2013) Regulation of flagellar motility during biofilm formation. *FEMS Microbiol Rev* **37**: 849–871.

Hall, C.W., and Mah, T.F. (2017) Molecular mechanisms of biofilm-based antibiotic resistance and tolerance in pathogenic bacteria. *FEMS Microbiol Rev* **41**: 276–301.

Hammes, F., and Egli, T. (2010) Cytometric methods for measuring bacteria in water: advantages, pitfalls and applications. *Anal Bioanal Chem* **397**: 1083–1095.

Han, J.E., Tang, K.F.J., Tran, L.H., and Lightner, D.V. (2015) Photorhabdus insect-related (Pir) toxin-like genes in a plasmid of *Vibrio parahaemolyticus*, the causative agent of acute hepatopancreatic necrosis disease (AHPND) of shrimp. *Dis Aquat Organ* **113**: 33–40.

Hansen, S.K., Rainey, P.B., Haagensen, J.A.J., and Molin, S. (2007) Evolution of species interactions in a biofilm community. *Nature* **445**: 533–536.

Hassan, A., Usman, J., Kaleem, F., Omair, M., Khalid, A., and Iqbal, M. (2011) Evaluation of different detection methods of biofilm formation in the clinical isolates. *Brazilian J Infect Dis* **15**: 305–311.

Hawkins, J.P., Geddes, B.A., and I.J., O. (2017) Common dyes used to determine bacterial polysaccharides on agar are affected by medium acidification. *Can J Microbiol Common* **63**: 559–562.

Henthorn, P., Zervos, P., Raducha, M., Harris, H., and Kadesch, T.O.M. (1988) Expression of a human placental alkaline phosphatase gene in transfected cells: use as a reporter for studies of gene expression. *Proc Nati Acad Sci USA* **85**: 6342–6346.

Jayaraman, R. (2011) Phase variation and adaptation in bacteria: A ' Red Queen's Race'. *Curr Sci* **100**: 1163–1171.

Kageyama, H., Tripathi, K., Rai, A.K., Cha-um, S., Waditee-Sirisattha, R., and Takabe, T. (2011) An alkaline phosphatase/phosphodiesterase, PhoD, induced by salt stress and secreted out of the cells of *Aphanothece halophytica*, a halotolerant cyanobacterium. *Appl Environ Microbiol* **77**: 5178–5183.

Kalivoda, E.J., Brothers, K.M., Stella, N.A., Schmitt, M.J., and Shanks, R.M.Q. (2013) Bacterial cyclic AMP-phosphodiesterase activity coordinates biofilm formation. *PLoS One* **8**: e71267.

Kato, C., Li, L., Nogi, Y., Nakamura, Y., and Tamaoka, J.I.N. (1998) Extremely barophilic bacteria isolated from the mariana trench, challenger deep, at a depth of 11, 000 meters. *Appl Environ Microbiol* **64**: 1510–1513.

Kemper, K., De Goeje, P.L., and Peeper, D.S. (2014) Phenotype switching: tumor cell plasticity as a resistance mechanism and target for therapy. *Cancer Res* **74**: 5937–5942.

Kent, A.G., Garcia, C.A., Martiny, A.C., and Biology, E. (2018) Increased biofilm formation due to high temperature adaptation in marine Roseobacter. *Nat Microbiol* **3**: 989–995.

Khan, A., Davlieva, M., Panesso, D., Rincon, S., Miller, W. R., Diaz, L., *et al*. (2019) Antimicrobial sensing coupled with cell membrane remodeling mediates antibiotic resistance and virulence in *Enterococcus faecalis*. *Proc Natl Acad Sci*: 1–8. https://doi.org/10.1073/pnas.1916037116

Kumar, V., Baruah, K., Nguyen, D.V., Smagghe, G., Vossen, E., and Bossier, P. (2018) Phloroglucinol mediated Hsp70 production in crustaceans: protection against *Vibrio parahaemolyticus* in *Artemia franciscana* and *Macrobrachium rosenbergii*. *Front Immunol* **9**: 1091.

Kumar, V., De Bels, L., Couck, L., Baruah, K., Bossier, P., and Van den Broeck, W. (2019a) PirABVP toxin binds to epithelial cells of the digestive tract and produce pathognomonic AHPND lesions in germ-free brine shrimp. *Toxins* **11**: 717.

Kumar, V., Viet, D., Baruah, K., and Bossier, P. (2019b) Probing the mechanism of VP AHPND extracellular proteins toxicity purified from *Vibrio parahaemolyticus* AHPND strain in germ-free *Artemia* test system. *Aquaculture* **504**: 414–419.

Laue, H., Schenk, A., Li, H., Lambertsen, L., Neu, T.R., Molin, S., and Ullrich, M.S. (2006) Contribution of alginate and levan production to biofilm formation by *Pseudomonas syringae*. *Microbiology* **152**: 2909–2918.

Lee, C.-T., Chen, I.-T., Yang, Y.-T., Ko, T.-P., Huang, Y.-T., Huang, J.-Y., *et al*. (2015) The opportunistic marine pathogen *Vibrio parahaemolyticus* becomes virulent by acquiring a plasmid that expresses a deadly toxin. *Proc Natl Acad Sci USA* **112**: 10798–10803.

Leid, J.G., Shirtliff, M.E., Costerton, J.W., and Stoodley, P. (2002) Human leukocytes adhere to, penetrate, and respond to *Staphylococcus aureus* biofilms. *Infect Immun* **70**: 6339–6345.

Leriche, V., Sibille, P., and Carpentier, B. (2000) Use of an enzyme-linked lectinsorbent assay to monitor the shift in polysaccharide composition in bacterial biofilms. *Appl Environ Microbiol* **66**: 1851–1856.

Li, P., Kinch, L.N., Ray, A., Dalia, A.B., Cong, Q., Nunan, L. M., *et al*. (2017) Acute hepatopancreatic necrosis disease-causing *Vibrio parahaemolyticus* strains maintain an antibacterial type VI secretion system with versatile effector repertoires. *Appl Environ Microbiol* **83**: e00737-17.

Liu, X., Long, D., You, H., Yang, D., Zhou, S., Zhang, S., *et al*. (2016) Phosphatidylcholine affects the secretion of the alkaline phosphatase PhoA in *Pseudomonas* strains. *Microbiol Res* **192**: 21–29.

Livak, K.J., and Schmittgen, T.D. (2001) Analysis of relative gene expression data using real-time quantitative PCR and the 2-ΔΔCT method. *Methods* **25**: 402–408.

Mancilla, E., Palacios-Morales, C.A., Córdova-Aguilar, M.S., Trujillo-Roldán, M.A., Ascanio, G., and Zenit, R. (2015) A hydrodynamic description of the flow behavior in shaken flasks. *Biochem Eng J* **99**: 61–66.

Mariana, N.S., Salman, S.A., and Zamberi, S. (2009) Evaluation of modified Congo red agar for detection of biofilm produced by clinical isolates of methicillin – resistance *Staphylococcus aureus*. *Afr J Microbiol Res* **3**: 330–338.

Mccarter, L.L. (2004) Dual flagellar systems enable motility under different circumstances. *J Mol Microbiol Biotechnol* **7**: 18–29.

Mlouka, M.A.B., Cousseau, T., and Martino, P.D. (2016) Application of fluorescently labelled lectins for the study of polysaccharides in biofilms with a focus on biofouling of nanofiltration membranes. *AIMS Mol Sci* **3**: 338–356.

Nalini, P., Ellaiah, P., Prabhakar, T., and Girijasankar, G. (2015) Microbial alkaline phosphatases in bioprocessing. *Int J Curr Microbiol Appl Sci* **4**: 384–396.

NCCLS. (2002) Performance standards for antimicrobial disk and dilution susceptibility tests for bacteria isolated from animals. In *Approved standard-second edition NCCLS document M31-A3*, Wayne, P. (ed). Wayne, Pennsylvania: National Committee for Clinical Laboratory Standards.

Nhan, D.T., Cam, D.T.V., Wille, M., Defoirdt, T., Bossier, P., and Sorgeloos, P. (2010) Quorum quenching bacteria

protect *Macrobrachium rosenbergii* larvae from *Vibrio harveyi* infection. *J Appl Microbiol* **109**: 1007–1016.

Nunan, L., Lightner, D., Pantoja, C., and Gomez-Jimenez, S. (2014) Detection of acute hepatopancreatic necrosis disease (AHPND) in Mexico. *Dis Aquat Organ* **111**: 81–86.

Park, A., Jeong, H., Lee, J., Kim, K.P., and Lee, C. (2011) Effect of shear stress on the formation of bacterial biofilm in a microfluidic channel. *Biochip J* **5**: 236–241.

Pfaffl, M.W. (2002) Relative expression software tool (REST (C)) for group-wise comparison and statistical analysis of relative expression results in real-time PCR. *Nucleic Acids Res* **30**: 36e–36e.

Phuoc, L.H., Defoirdt, T., Sorgeloos, P., and Bossier, P. (2009) Virulence of luminescent and non-luminescent isogenic vibrios towards gnotobiotic *Artemia franciscana* larvae and specific pathogen-free *Litopenaeus vannamei* shrimp. *J Appl Microbiol* **106**: 1388–1396.

Poelwijk, F.J., Kiviet, D.J., and Tans, S.J. (2006) Evolutionary potential of a duplicated repressor-operator pair: simulating pathways using mutation data. *PLoS Comput Biol* **2**: e58.

Rahman, M.M., Wille, M., Cavalli, R.O., Sorgeloos, P., and Clegg, J.S. (2004) Induced thermotolerance and stress resistance in larvae of the freshwater prawn, *Macrobrachium rosenbergii* (de Man, 1879). *Aquaculture* **230**: 569–579.

Rainey, P.B., and Travisano, M. (1998) Adaptive radiation ina heterogeneousenvironment. *Nature* **394**: 69–72.

Rossignol, G., Sperandio, D., Guerillon, J., Poc, C.D., and Soum-soutera, E. (2009) Phenotypic variation in the *Pseudomonas fluorescens* clinical strain MFN1032. *Res Microbiol* **160**: 337–344.

Roy, S., Kumar, V., Bossier, P., Norouzitallab, P., and Vanrompay, D. (2019) Phloroglucinol treatment induces transgenerational epigenetic inherited resistance against vibrio infections and thermal stress in a brine shrimp (*Artemia franciscana*) model. *Front Immunol* **10**: 2745.

Scott, M., Mateescu, E.M., Zhang, Z., and Hwa, T. (2010) Interdependence of cell growth and gene expression: origins and consequences. *Science* **330**: 1099–1103.

Shikuma, N.J., Davis, K.R., Fong, J.N.C., and Yildiz, F.H. (2013) The transcriptional regulator, CosR, controls compatible solute biosynthesis and transport, motility and biofilm formation in *Vibrio cholerae*. *Environ Microbiol* **15**: 1387–1399.

Singh, S., Singh, S.K., Chowdhury, I., and Singh, R. (2017) Understanding the mechanism of bacterial biofilms resistance to antimicrobial agents. *Open Microbiol J* **11**: 53–62.

Sirikharin, R., Taengchaiyaphum, S., Sanguanrut, P., Chi, T. D., Mavichak, R., Proespraiwong, P., *et al*. (2015) Characterization and PCR detection of binary, pir-like toxins from *Vibrio parahaemolyticus* isolates that cause acute hepatopancreatic necrosis disease (AHPND) in shrimp. *PLoS One* **10**: 1–16.

Sirikharin, R., Taengchaiyaphum, S., Sritunyalucksana, K., Thitamadee, S., Flegel, T.W., and Mavichak, R. (2014) A new and improved PCR method for detection of AHPND bacteria. 7–9.

Sousa, A.M., Machado, I., and Pereira, M.O. (2011) Phenotypic switching: an opportunity to bacteria thrive. In *Communicating Current Research and Technological Advances*. Spain: Formatex, pp. 252–262.

Spiers, A.J., Kahn, S.G., Bohannon, J., Travisano, M., and Rainey, P.B. (2002) Adaptive divergence in experimental populations of *Pseudomonas fluorescens*. I. Genetic and phenotypic bases of wrinkly spreader fitness. *Genetics* **161**: 33–46.

Sultana, T., Haque, M., Salam, M., and Alam, M. (2017) Effect of aeration on growth and production of fish in intensive aquaculture system in earthen ponds. *J Bangladesh Agric Univ* **15**: 113–122.

Suong, N.T., Van Hao, N., Van Sang, N., Hung, N.D., Tinh, N.T.N., Phuoc, L.H., *et al*. (2017) The impact of catecholamine sensing on the virulence of *Vibrio parahaemolyticus* causing acute hepatopancreatic necrosis disease (AHPND). *Aquaculture* **470**: 190–195.

Tadrowski, A.C., Evans, M.R., and Waclaw, B. (2018) Phenotypic switching can speed up microbial evolution. *Sci Rep* **8**: 8941.

Thomen, P., Robert, J., Monmeyran, A., Bitbol, A., and Henry, N. (2017) Bacterial biofilm under flow: first a physical struggle to stay, then a matter of breathing. *PLoS One* **12**: e0175197.

Tran, L., Nunan, L., Redman, R.M., Mohney, L.L., Pantoja, C.R., Fitzsimmons, K., and Lightner, D.V. (2013) Determination of the infectious nature of the agent of acute hepatopancreatic necrosis syndrome affecting penaeid shrimp. *Dis Aquat Organ* **105**: 45–55.

Velázquez-Hernández, M.L., Baizabal-Aguirre, V.M., Bravo-Patiño, A., Cajero-Juárez, M., Chávez-Moctezuma, M.P., and Valdez-Alarcón, J.J. (2009) Microbial fructosyltransferases and the role of fructans. *J Appl Microbiol* **106**: 1763–1778.

Vilain, S., Cosette, P., Junter, G.-A., and Jouenne, T. (2002) Phosphate deprivation is associated with high resistance to latamoxef of gel-entrapped, sessile-like *Escherichia coli* cells. *J Antimicrob Chemother* **49**: 315–320.

De Visser, J.A.G.M., and Krug, J. (2014) Empirical fitness landscapes and the predictability of evolution. *Nat Rev Genetics* **15**: 480–490.

Vuong, C., Kocianova, S., Voyich, J.M., Yao, Y., Fischer, E. R., Deleo, F.R., and Otto, M. (2004) A crucial role for exopolysaccharide modification in bacterial biofilm formation, immune evasion, and virulence. *J Biol Chem* **279**: 54881–54886.

Watnick, P. (2000) Biofilm, city of microbes. *J Bacteriol* **182**: 2675–2679.

Welker, T.L., Overturf, K., and Abernathy, J. (2019) Effect of aeration and oxygenation on growth and survival of rainbow trout in a commercial serial-pass, flow-through raceway system. *Aqua Reports* **14**: 100194.

Van Der Woude, M.W. (2006) Re-examining the role and random nature of phase variation. *FEMS Microbiol Lett* **254**: 190–197.

Wu, J.R., Shien, J.H., Shieh, H.K., Hu, C.C., Gong, S.R., Chen, L.Y., and Chang, P.C. (2007) Cloning of the gene and characterization of the enzymatic properties of the monomeric alkaline phosphatase (PhoX) from *Pasteurella*

multocida strain X-73. *FEMS Microbiol Lett* **267**: 113–120.

Yang, Q., and Defoirdt, T. (2015) Quorum sensing positively regulates flagellar motility in pathogenic *Vibrio harveyi*. *Environ Microbiol* **17**: 960–968.

Yayanos, A., Dietz, A.S., and Boxtel, R.V. (1981) Obligately barophilic bacterium from the Mariana Trench. *Proc Natl Acad Sci U S A* **78**: 5212–5215.

Zhang, L., Weng, Y., Wu, Y., Wang, X., Yin, Z., Yang, H., *et al*. (2018) H-NS is an activator of exopolysaccharide biosynthesis genes transcription in *Vibrio parahaemolyticus*. *Microb Pathog* **116**: 164–167.

Zhou, M., Guo, Z., Yang, Y., Duan, Q., Zhang, Q., Yao, F., *et al*. (2014) Flagellin and F4 fimbriae have opposite effects on biofilm formation and quorum sensing in F4ac + enterotoxigenic *Escherichia coli*. *Vet Microbiol* **168**: 148–153.

Zidour, M., Chevalier, M., Belguesmia, Y., Cudennec, B., Grard, T., Drider, D., *et al*. (2017) Isolation and characterization of bacteria colonizing *Acartia tonsa* copepod eggs and displaying antagonist effects against *Vibrio anguillarum*, *Vibrio alginolyticus* and other pathogenic strains. *Front Microbiol* **8**: 1–13.

Supporting Information

Additional Supporting Information may be found in the online version of this article at the publisher's web-site:

Fig. S1. Floccule formation increases the resistance of AHPND *Vibrio parahaemolyticus* M0904 strain to antibiotics

Fig. S2. MS/MS spectrum of peptide

Fig. S3. Floccule formation decreases the toxicity of AHPND *Vibrio parahaemolyticus* M0904 strain in *Macrobrachium rosenbergii* larvae

Fig. S4. Agarose gel of PCR amplicon from *Vibrio parahaemolyticus* M0904 strain using AP3 method

Table S1. iBAQ ratio of the identified proteins from gel band (The mass spectrometry proteomics data have been deposited to the ProteomeXchange Consortium via the PRIDE partner repository with the dataset identifier PXD015617)

Table S2. Types of lectins used in the study for flow cytometry

Table S3. AP3 primers used in this study

Table S4. Specific primers and their sequence used for reverse transcriptase real-time PCR